Dissipatively dressed quasiparticles in boundary-driven integrable spin chains

Vladislav Popkov [1,2,*] Xin Zhang [3,*] Carlo Presilla [4,5] and Tomaž Prosen [1,6]

[1]*Faculty of Mathematics and Physics, University of Ljubljana, Jadranska 19, SI-1000 Ljubljana, Slovenia*

[2]*Department of Physics, University of Wuppertal, Gaussstraße 20, 42119 Wuppertal, Germany*

[3]*Beijing National Laboratory for Condensed Matter Physics, Institute of Physics, Chinese Academy of Sciences, Beijing 100190, China*

[4]*Dipartimento di Matematica, Università di Roma La Sapienza, Piazzale Aldo Moro 5, Roma 00185, Italy*

[5]*Istituto Nazionale di Fisica Nucleare, Sezione di Roma 1, Roma 00185, Italy*

[6]*Institute of Mathematics, Physics and Mechanics, Jadranska 19, SI-1000 Ljubljana, Slovenia*

(Received 26 August 2024; revised 5 December 2025; accepted 3 February 2026; published 16 March 2026)

The nonequilibrium steady state (NESS) of integrable spin chains experiencing strong boundary dissipation is accounted for by introducing quasiparticles with a renormalized—dissipatively dressed—dispersion relation. This allows us to evaluate the spectrum of the NESS in terms of the Bethe Ansatz equations for a related coherent system that has the same set of eigenstates, the so-called dissipation-projected Hamiltonian. We find explicit analytic expressions for the dressed energies of the *XXX* and *XXZ* models with effective, i.e., induced by the dissipation, diagonal boundary fields, which are $U(1)$ invariant, as well as the *XXZ* and *XYZ* models with effective nondiagonal boundary fields. In all cases, the dissipative dressing generates an extra singularity in the dispersion relation, substantially altering the NESS spectrum with respect to the spectrum of the corresponding coherent model.

DOI: 10.1103/2zbl-3twm

I. INTRODUCTION

The notion of quasiparticles is a fundamental concept in regular many-body systems irrespective of whether they are integrable or not. Examples of quasiparticles are phonons in crystals and magnons in magnetic materials. In integrable continuous theories with nonlinearities (e.g., in Korteweg–de Vries or sine-Gordon models), stable quasiparticles are solitons, or solitary waves which are spatially localized: after a collision they retain their original velocities and shapes, the net result of the scattering being just a shifting of their world lines. Quasiparticles of integrable quantum interacting many-body systems on a lattice also possess special properties with regard to their multiple scattering: the multiple quasiparticle collision can be factorized in terms of a two-body scattering matrix. Every eigenstate in an integrable quantum system can be viewed as consisting of quasiparticles. Most prominently, the eigenenergy of any eigenstate is obtainable by summing individual energies of all quasiparticles it contains $E_\alpha = \sum_j \epsilon(u_{j,\alpha})$, where $u_{j,\alpha}$ is a set of admissible rapidities and $\epsilon(u)$ is a dispersion relation. The dispersion relation $\epsilon(u)$ is a fundamental property of quasiparticles, and it is very robust; e.g. the dispersion does not depend on boundary conditions, temperature, or system size.

The purpose of our study is to establish a relation between two fundamental quantities from seemingly very different fields: the spectrum E_α of a coherent (closed) integrable many-body system, from one side, and the spectrum λ_α of a nonequilibrium steady state of the "same" open quantum system in contact with a locally acting dissipative bath, from another side. In more details, we will demonstrate that under a proper choice of the dissipation, there exists a one-to-one correspondence between the two spectra, namely, that $\ln \lambda_\alpha = \sum_j \tilde{\epsilon}(u_{j,\alpha})$, where $u_{j,\alpha}$ is exactly the same set of admissible rapidities, constituting the spectrum of a coherent system $E_\alpha = \sum_j \epsilon(u_{j,\alpha})$, and $\tilde{\epsilon}(u)$ is a renormalized dispersion (we refer to it as a *dissipatively dressed dispersion relation*). The existence of a renormalized dispersion relation relating coherent (unitary) and strongly incoherent (dissipative) systems seems rather counterintuitive; however, its general validity lies beyond what we are currently able to prove.

We compare an equilibrium Gibbs state ρ_{Gibbs} of a quantum integrable many-body system, from one side, and a nonequilibrium steady state ρ_{NESS} of "almost the same" system, with a part of degrees of freedom coupled to a dissipative bath, from the other side. The Gibbs state is

$$\rho_{\text{Gibbs}} = \frac{1}{Z}\sum_\alpha e^{-\beta E_\alpha}|\alpha\rangle\langle\alpha|,$$
$$E_\alpha = \sum_j \epsilon(u_{j,\alpha}), \tag{1}$$

where $\epsilon(u)$ is the dispersion relation of the quasiparticles, and $u_{j,\alpha}$ are the admissible rapidities, obtained via the quantization conditions, namely, a set of Bethe Ansatz equations (BAEs) obtainable by different methods [1–5]. The type of quasiparticles and their number depend on the model and

*These authors contributed equally to this work.

the intrinsic quantum numbers characterizing the microstates $\{|\alpha\rangle\}$.

In the dissipative setup, we consider a "similar" quantum system, with boundary degrees of freedom coupled to a dissipative bath, described via a Lindblad Master equation. This leads to a nonunitary dynamics of a reduced density matrix $\rho(t)$, which relaxes to a (unique) nonequilibrium steady state (NESS), $\lim_{t\to\infty}\rho(t)=\rho_{\rm NESS}$. In general, there is no reason to expect any close relation between the Gibbs state (1) and the NESS.

The purpose of this article is to show, that under certain conditions, (A) the NESS has the same set of eigenstates $|\alpha\rangle$ as in Eq. (1), i.e.,

$$[\rho_{\rm NESS},\rho_{\rm Gibbs}]=0, \tag{2}$$

and (B) the effective energies $\tilde{E}_\alpha$ are described by exactly the same quasiparticle content as E_α; i.e., they are given by the sum of the same set of quasiparticles as in Eq. (1), but with renormalized—"dissipatively dressed"—dispersion relation $\epsilon(u)\to\tilde{\epsilon}(u)$:

$$\rho_{\rm NESS}=\frac{1}{\tilde{Z}}\sum_\alpha e^{-\tilde{E}_\alpha}|\alpha\rangle\langle\alpha|, \tag{3}$$

$$\tilde{E}_\alpha=\sum_j\tilde{\epsilon}(u_{j,\alpha}). \tag{4}$$

Relation (4) is very surprising: it suggests that the notion of Bethe quasiparticles (an intrinsic property of a coherent integrable system) can, under certain conditions, be preserved under dissipation, at least with respect to its steady state (NESS).

The following sections serve to explain the relation between coherent and dissipation-affected quantum systems in detail. In Appendix A we sketch a derivation of the Lindblad master equation starting from a brick-wall qubit circuit. Appendixes B, C, and D contain some details and Tables for *XXZ* and *XYZ* models with chiral invariant subspaces.

We note that this is a companion paper expanding on a recent exact result [6], here including heuristic and numerical evidence in a broader family of integrable models and dissipation setups.

II. INTEGRABLE SPIN CHAINS WITH BOUNDARY FIELDS AND BOUNDARY-DRIVEN SPIN CHAINS

Our coherent system is a general open spin-$\frac{1}{2}$ chain described by a nearest-neighbor Heisenberg Hamiltonian with general boundary fields $h_1=\vec{h}_1\cdot\vec{\sigma}_1$ and $h_N=\vec{h}_N\cdot\vec{\sigma}_N$,

$$H=H_{\rm bulk}+h_1+h_N, \tag{5}$$

$$H_{\rm bulk}=\sum_{n=1}^{N-1}\vec{\sigma}_n\cdot\hat{J}\vec{\sigma}_{n+1},\quad \hat{J}=\mathrm{diag}(J_x,J_y,J_z). \tag{6}$$

It is known (see Refs. [7,8]) that the above system is integrable for any choice of $J_x,J_y,J_z,\vec{h}_1,\vec{h}_N$. More popular examples of *XXZ* and *XXX* models result from reductions $J_x=J_y$ and $J_x=J_y=J_z$. As such, any eigenstate of Eq. (5) has a quasiparticle content, with admissible values of the rapidities in Eq. (1), given by the respective Bethe Ansatz equations [8]. Later on, the boundary fields will be specified.

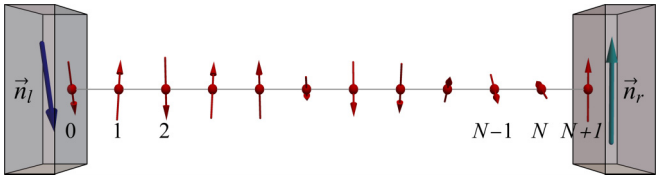

FIG. 1. Schematic picture of the dissipative setup. The boundary spins are fixed by dissipation, while the internal spins follow effective dynamics (13), consisting of fast coherent dynamics (5) and slow relaxation dynamics (17) towards the NESS. Here, $\vec{n}_l$ and $\vec{n}_r$ are the unit polarization vectors of the targeted states $|\psi_l\rangle$ and $|\psi_r\rangle$.

On the dissipative side, our scenario is as follows: we have a spin chain of $N+2$ sites (note that there are two extra sites with respect to the coherent system above), described by the Hamiltonian $H=\sum_{n=0}^{N}\vec{\sigma}_n\cdot\hat{J}\vec{\sigma}_{n+1}$ [the same Hamiltonian as in Eq. (6) with two sites added], in which the edge spins, those at positions $n=0$ and $n=N+1$, are projected on pure qubit states ρ_l,ρ_r, respectively, by coupling to a dissipative Lindblad bath. A Schematic picture is given in Fig. 1.

The time evolution of the reduced density matrix is described by the Lindblad Master equation:

$$\frac{\partial\boldsymbol{\rho}(\Gamma,t)}{\partial t}=-i[H,\boldsymbol{\rho}]+\Gamma(\mathcal{D}_{L_1}[\boldsymbol{\rho}]+\mathcal{D}_{L_2}[\boldsymbol{\rho}]), \tag{7}$$

$$\mathcal{D}_L[\boldsymbol{\rho}]=L\boldsymbol{\rho}L^\dagger-\frac{1}{2}(L^\dagger L\boldsymbol{\rho}+\boldsymbol{\rho}L^\dagger L). \tag{8}$$

The Lindblad operators can be conveniently chosen in a form $L_1=|\psi_l\rangle\langle\psi_l|^\perp\otimes I^{\otimes_{N+1}}$, $L_2=I^{\otimes_{N+1}}\otimes|\psi_r\rangle\langle\psi_r|^\perp$, where $\langle\psi^\perp|\psi\rangle=0$. Indeed the Lindblad dissipators $\mathcal{D}_{L_1}$ and $\mathcal{D}_{L_2}$ will then promote the relaxation of edge spins to targeted pure states $|\psi_{l,r}\rangle$, with typical relaxation time $\tau_{\rm boundary}=O(1/\Gamma)$. We will consider the case when $\tau_{\rm boundary}$ is much smaller than a typical time needed for the bulk relaxation, $\tau_{\rm boundary}\ll\tau_{\rm bulk}$, the so-called quantum Zeno (QZ) regime. Note that Γ need not be necessarily very large to reach the QZ regime; e.g., for *XXX* bulk Hamiltonian $J_x=J_y=J_z$ the effective $\Gamma=O(N^{-1})$ is shown in Ref. [9].

The quantum Zeno regime with arbitrary Γ can be realized by a protocol of repeated interactions [10]. In this protocol, the edge spin is repeatedly brought in contact with a freshly polarized magnet (see, e.g., Appendix A of Ref. [11] for an explicit protocol and the derivation of Eq. (7). Alternatively, an instantaneous projection of a single qubit can be achieved by applying a so-called reset gate [12]: the gate simply resets a qubit state to a desired qubit state at each application. In Appendix A we give a derivation of Eq. (7) from a qubit circuit protocol.

The fast relaxation of the edge spins in the QZ regime constrains the reduced density matrix of Eq. (7) to an approximately factorized form [13] $\boldsymbol{\rho}(\Gamma,t)=\rho_l\otimes\rho(\Gamma,t)\otimes\rho_r+O(1/\Gamma)$ for $t\gg1/\Gamma$, where $\rho(t)\approx\mathrm{tr}_{0,N+1}\boldsymbol{\rho}(t)$ is the reduced density matrix after the tracing over the part directly affected by the dissipation [13], i.e., the reduced density matrix of interior spins.

Moreover, it can be shown that $\rho(\Gamma,t)$ *commutes* with Hamiltonian (5) for suitably chosen boundary fields h_1,h_N [14], confirming that the time evolution of $\boldsymbol{\rho}(\Gamma,t)$ for $t\gg1/\Gamma$ is approximately coherent [13].

For our purposes it is enough to demonstrate that $\lim_{\Gamma\to\infty}\lim_{t\to\infty}\rho(t)=\rho_{\rm NESS}$ satisfies

$$[\rho_{\rm NESS}, H_{\rm bulk}+h_1+h_N]=0, \tag{9}$$

$$h_1=\vec{\sigma}_1\cdot\hat{J}\vec{n}_l\equiv\sum_{\alpha=x,y,z}J_\alpha n_l^\alpha\sigma_1^\alpha, \tag{10}$$

$$h_N=\vec{\sigma}_N\cdot\hat{J}\vec{n}_r, \tag{11}$$

where $H_{\rm bulk}$ is given by Eq. (6), and $\vec{n}_l,\vec{n}_r$ are unit vectors of polarizations of the targeted states $|\psi_l\rangle, |\psi_r\rangle$. For a proof, we expand the steady-state solution $\boldsymbol{\rho}(\Gamma)$ of Eq. (7) in powers of $1/\Gamma$, $\boldsymbol{\rho}(\Gamma)=\rho_0+\Gamma^{-1}\rho_1+\Gamma^{-2}\rho_2+\cdots$. Substituting into Eq. (7), we obtain a set of conditions $i[H,\rho_k]=(\mathcal{D}_{L_1}+\mathcal{D}_{L_2})[\rho_{k+1}]$, for $k=0,1,\ldots$. These conditions are nontrivial since the operator $(\mathcal{D}_{L_1}+\mathcal{D}_{L_2})$ has a nonzero kernel of the form $\rho_l\otimes X\otimes\rho_r$, where X is an arbitrary matrix. In all orders, the necessary and sufficient condition for the existence of ρ_{n+1} is $\mathrm{tr}_{0,N+1}[H,\rho_n]=0$. In the leading order $n=0$, a substitution of $\rho_0=\rho_l\otimes\rho_{\rm NESS}\otimes\rho_r$ into $\mathrm{tr}_{0,N+1}[H,\rho_0]=0$ leads to Eqs. (9)–(11). Hamiltonian (9) is called a dissipation-projected Hamiltonian [13]. Thus, we obtain property A [Eq. (2)].

Remark 1. We proved that the eigenstates of the Zeno NESS for boundary-driven integrable spin chains are those of an integrable Hamiltonian with fine-tuned boundary fields h_1, h_N. Note that due to Eqs. (10) and (11) the conditions

$$\min_\alpha J_\alpha\leqslant\|h_1\|,\quad \|h_N\|\leqslant\max_\alpha J_\alpha, \tag{12}$$

are always satisfied, restricting the norm of "permissible" boundary fields in Eq. (9).

To show property B is more involved, it requires, to start with, a description of the relaxation mechanism of internal spins toward the steady state, $\rho(t)\to\rho_{\rm NESS}$ for $t\gg 1/\Gamma$. This requires writing a Dyson expansion of the time-dependent solution of the Lindblad master equation (7) using $1/\Gamma\ll 1$ as a perturbation parameter. The procedure is explained in detail in Refs. [13,14], while here we give an outline. The first two orders of the Dyson expansion yield an effective Lindblad Master equation for internal spins, $\rho(t)=\mathrm{tr}_{0,N+1}\boldsymbol{\rho}(t)$ for $t\gg 1/\Gamma$ [14],

$$\frac{\partial\rho(\Gamma,t)}{\partial t}=-i[H_D,\rho]+\frac{1}{\Gamma}(\mathcal{D}_{g_l}[\rho]+\mathcal{D}_{g_r}[\rho]), \tag{13}$$

where $H_D\equiv H_{\rm bulk}+h_1+h_N$ is the dissipation-projected Hamiltonian, and g_l, g_r are effective Lindblad operators, explicitly given by

$$\begin{aligned} g_l&=\mathrm{tr}_{0,N+1}[(|\psi_l\rangle\langle\psi_l^\perp|\otimes I^{\otimes_{N+1}})H]\\ &=\mathrm{tr}_0[\langle\psi_l^\perp|\vec{\sigma}|\psi_l\rangle\otimes\hat{J}\vec{\sigma}]\otimes I^{\otimes_{N-1}}, \end{aligned} \tag{14}$$

$$\begin{aligned} g_r&=\mathrm{tr}_{0,N+1}[(I^{\otimes_{N+1}}\otimes|\psi_r\rangle\langle\psi_r^\perp|)H]\\ &=I^{\otimes_{N-1}}\otimes\mathrm{tr}_1[\hat{J}\vec{\sigma}\otimes\langle\psi_r^\perp|\vec{\sigma}|\psi_r\rangle]. \end{aligned} \tag{15}$$

Note that the dissipative part in Eq. (13) is of the order $1/\Gamma$, in contrast to Eq. (7), where it is of order Γ. Thus, indeed, the effective time evolution of the bulk is approximately coherent while the relaxation is proportional to $1/\Gamma$.

Due to Eq. (9) the NESS can be written in the basis of eigenstates $|\alpha\rangle$ of $H_{\rm bulk}+h_1+h_N$,

$$\rho_{\rm NESS}=\sum_\alpha\nu_\alpha|\alpha\rangle\langle\alpha|. \tag{16}$$

Assuming orthonormality $\langle\alpha|\beta\rangle=\delta_{\alpha,\beta}$, and multiplying Eq. (13) by $\langle\alpha|$ from the left and by $|\alpha\rangle$ from the right, one obtains a closed system for the populations $\nu_\alpha(t)=\langle\alpha|\rho(t)|\alpha\rangle$:

$$\Gamma\frac{\partial\nu_\alpha(t)}{\partial t}=\sum_{\beta\neq\alpha}w_{\beta\alpha}\nu_\beta-\nu_\alpha\sum_{\beta\neq\alpha}w_{\alpha\beta},\quad \alpha=1,2,\ldots, \tag{17}$$

$$w_{\beta\alpha}=|\langle\alpha|g_l|\beta\rangle|^2+|\langle\alpha|g_r|\beta\rangle|^2. \tag{18}$$

The Quantities $\nu_\alpha(t)=\langle\alpha|\rho(t)|\alpha\rangle$ are real, non-negative, and sum up to 1 [due to normalization $\mathrm{tr}\rho(t)=1$], which allows to interpret them as probabilities and Eq. (17) as a classical master equation for an auxiliary classical Markov process, with renormalized rates $w_{\alpha\beta}$. The stationary solution of the auxiliary Markov process (17), i.e., the solution of

$$\sum_{\beta\neq\alpha}w_{\beta\alpha}\nu_\beta-\nu_\alpha\sum_{\beta\neq\alpha}w_{\alpha\beta}=0,\quad \alpha=1,2,\ldots, \tag{19}$$

where all $\nu_\alpha\geqslant 0$ due to the Perron-Frobenius theorem, yields the NESS spectrum $\{\nu_\alpha\}\equiv\{e^{-\tilde{E}_\alpha}/\tilde{Z}\}$. From Eq. (19) we can find the Zeno NESS for various $\hat{J}$, $\vec{n}_l$, and $\vec{n}_r$. Numerically, in all cases we observe the Kolmogorov relation for the rates $w_{\alpha\beta}$:

$$w_{\alpha\beta}w_{\beta\gamma}w_{\gamma\alpha}=w_{\alpha\gamma}w_{\gamma\beta}w_{\beta\alpha}. \tag{20}$$

A direct consequence of the Kolmogorov relation is the detailed balance property of the solution of Eq. (19),

$$\nu_\alpha w_{\alpha\beta}=\nu_\beta w_{\beta\alpha}. \tag{21}$$

Remark 2. The Kolmogorov relation [Eq. (20)] is only satisfied for pure targeted boundary states, i.e., for boundary fields obeying Eqs. (10) and (11) with $|\vec{n}_l|=|\vec{n}_r|=1$. It is remarkable for our purpose since it gives a direct way to find the NESS spectrum ν_α, via Eq. (21), avoiding solution of the full linear system (19) which is in general of exponential complexity (in system size N). Even though Eq. (20) is postulated, in all specific cases its validity can be checked, or proved, *a posteriori*. Note that due to Eq. (21), the problem of finding Zeno NESS eigenvalues ν_α reduces to a problem of finding ratios of certain correlations of eigenstates of integrable model (5), i.e., to a problem widely studied in the literature.

We discuss several explicit examples, for which we find the NESS spectrum $\{\nu_\alpha\}=\{\exp(-\tilde{E}_\alpha)/\tilde{Z}\}$, and establish the dissipative dressing property (4):

(i) *XXX* and *XXZ* models with boundary qubits targeted in the direction of the z axis; (ii) *XXZ* model with boundary targeting specific polarization in the *XY* plane; (iii) *XYZ* model with boundary targeting in specific directions. In case (i), the corresponding effective Hamiltonian is $U(1)$ symmetric, and in case (ii) the $U(1)$ symmetry is broken by nondiagonal boundary fields. Finally, case (iii) provides evidence for the existence of dissipatively dressed quasiparticles in the most general fully anisotropic version of the Heisenberg exchange interaction, i.e., for an *XYZ* spin chain, where $U(1)$ symmetry is broken already at the level of the bulk Hamiltonian. The original and modified dispersion relations, for all three cases

(i), (ii), and (iii), constitute our main results and are listed in the next section.

III. DISSIPATIVE DRESSING OF QUASIPARTICLE DISPERSION: *XXX*, *XXZ*, AND *XYZ* MODELS WITH BOUNDARY DRIVING

XXX model with sink and source. The dissipation-projected Hamiltonian with isotropic bulk exchange interaction and boundary fields along the z axis $h_1 = -\sigma_1^z$, $h_N = \sigma_N^z$,

$$H_D = \sum_{n=1}^{N-1} \vec{\sigma}_n \cdot \vec{\sigma}_{n+1} - \sigma_1^z + \sigma_N^z, \tag{22}$$

describes the effective dynamics (13) of internal spins in an isotropic Heisenberg model of length $N+2$ where the first and the last spin are projected onto the spin-down state $|\downarrow\rangle$ and spin-up state $|\uparrow\rangle$, respectively, i.e., $\vec{n}_l = (0,0,-1)$, $\vec{n}_r = (0,0,1)$, in accordance with Eqs. (10) and (11). The $U(1)$ symmetry renders Hamiltonian (22) block-diagonalizable within blocks of fixed magnetization. The eigenstates $|\alpha\rangle$ of H_D belonging to the block with magnetization $N-2M$ have energies (eigenvalues) $E_\alpha = N - 1 + \sum_{j=1}^M \epsilon(u_{j,\alpha})$, where $u_{j,\alpha}$, $j = 1, \ldots, M$, are Bethe rapidities, satisfying the Bethe Ansatz relations

$$\frac{u_j^{[-3]}}{u_j^{[+3]}} \left(\frac{u_j^{[+1]}}{u_j^{[-1]}} \right)^{2N+1} = \prod_{\substack{k=1 \\ k\neq j}}^{M} \prod_{\sigma=\pm 1} \frac{(u_j + \sigma u_k)^{[+2]}}{(u_j + \sigma u_k)^{[-2]}}, \tag{23}$$

in which we defined

$$u^{[q]} \equiv u + iq/2, \tag{24}$$

and $\epsilon(u)$ is the standard dispersion relation,

$$\epsilon(u) = -\frac{2}{u^2 + \frac{1}{4}}. \tag{25}$$

The NESS of the spin chain with boundary dissipation (Fig. 1) has the form $|\downarrow\rangle\langle\downarrow| \otimes \rho_{\rm NESS} \otimes |\uparrow\rangle\langle\uparrow|$ with $\rho_{\rm NESS}$ given by Eq. (4), $\tilde{E}_\alpha = \sum_{j=1}^M \tilde{\epsilon}(u_{j,\alpha})$, and the modified, or dissipatively dressed, dispersion relation

$$\tilde{E}_\alpha = \sum_{j=1}^{M} \tilde{\epsilon}(u_{j,\alpha}),$$

$$\tilde{\epsilon}(u) = \ln \left| \frac{u^2 + \frac{9}{4}}{u^2 + \frac{1}{4}} \right| = \ln |1 - \epsilon(u)|, \tag{26}$$

where $u_{j,\alpha}$ are given by the same BAE (23).

Note that the dispersion (26) contains singularities: a singularity at the point $u = \pm i/2$ [inherited from the original quasiparticle dispersion (25)], gets "dressed" with the second singularity $u = \pm 3i/2$, which is generated by the dissipation. We call this phenomenon a "dissipative dressing of the quasiparticle dispersion," and the corresponding function a "dissipatively dressed dispersion." Qualitatively the same mechanism is observed for other scenarios (see below).

XXZ model with sink and source. Our next example is the *XXZ* model:

$$H_D = \sum_{n=1}^{N-1} \vec{\sigma}_n \cdot \hat{J} \vec{\sigma}_{n+1} + h_1 + h_N, \tag{27}$$

$$\hat{J} = \mathrm{diag}(1, 1, \Delta), \quad h_1 = -\sigma_1^z \Delta, \quad h_N = \sigma_N^z \Delta. \tag{28}$$

The Hamiltonian in Eq. (27) gives an effective dynamics (13) for an *XXZ* spin chain with z anisotropy Δ and leftmost (rightmost) spins projected onto states $|\downarrow\rangle$ ($|\uparrow\rangle$), respectively, i.e., $\vec{n}_l = (0,0,-1)$, $\vec{n}_r = (0,0,1)$ [see Eqs. (10) and (11)]. For $\Delta = 1$, Eq. (27) reduces to Eq. (22). Like Eq. (22), Hamiltonian (27) possesses $U(1)$ symmetry. The spectrum of coherent model (27) is given by $E_\alpha = (N-1)\Delta + \sum_{j=1}^M \epsilon(u_{j,\alpha})$, where $\{u_{j,\alpha}\}$ satisfy Eq. (23) with the replacement

$$u^{[k]} \equiv \sinh(u + ik\gamma/2), \tag{29}$$

where $\cos\gamma = \Delta$ (see the pioneering paper of Sklyanin [15]). The NESS spectrum of the dissipation-driven model in Fig. 1 is given by $\{\nu_\alpha \propto \exp(-\tilde{E}_\alpha)\}$, $\tilde{E}_\alpha = \sum_{j=1}^M \tilde{\epsilon}(u_{j,\alpha})$.

The original and dissipatively dressed dispersions are, respectively (see Ref. [6])

$$\epsilon(u) = \frac{-2\sin^2\gamma}{\sinh\left(u + \frac{i\gamma}{2}\right)\sinh\left(u - \frac{i\gamma}{2}\right)}, \tag{30}$$

$$\tilde{\epsilon}(u) = \ln \left| \frac{\sinh\left(u + \frac{3i\gamma}{2}\right)\ \sinh\left(u - \frac{3i\gamma}{2}\right)}{\sinh\left(u + \frac{i\gamma}{2}\right)\ \sinh\left(u - \frac{i\gamma}{2}\right)} \right|$$

$$= \ln|1 - \epsilon(u)\Delta|. \tag{31}$$

Setting $\gamma \to \delta$, $u \to \delta u$, and letting $\delta \to 0$ one recovers the result for the isotropic Heisenberg model [Eq. (26)].

XXZ model with chiral invariant subspace. An *XXZ* Hamiltonian [Eq. (27)] with nondiagonal boundary fields

$$h_1 = \sigma_1^x, \quad h_N = \sigma_N^x \cos\varphi(M) + \sigma_N^y \sin\varphi(M), \tag{32}$$

$$\varphi(M) = (N + 1 - 2M)\gamma, \quad \cos\gamma = \Delta, \tag{33}$$

gives an effective dynamics (13) for an *XXZ* spin chain with anisotropy Δ and leftmost and rightmost spins projected onto fully polarized states in the XY plane $\vec{n}_l = (1,0,0)$ $\vec{n}_r = (\cos\varphi(M), \sin\varphi(M), 0)$. It was shown in Refs. [16,17] that for integer values $M = 0, 1, \ldots, N+1$, Hamiltonian (32) has a chiral invariant subspace G_M. G_M is spanned by pieces of spin helices of the period $2\pi/\gamma$, and of the same helicity sign, and its dimension is $d_M = \binom{N+1}{M}$.

The Gibbs state restricted to the invariant subspace G_M has the form of Eq. (1) with $\alpha = 1, \ldots, d_M$ and $j = 1, \ldots, M$. The integer M counts the number of kinks and is analogous to the number of spin-down arrows in the $U(1)$-invariant case [Eq. (27)]: each state $|\alpha\rangle$ is parametrized via M Bethe rapidities $u_{j,\alpha}$, satisfy Bethe Ansatz equations:

$$\left[\frac{\sinh\left(u_j + \frac{i\gamma}{2}\right)}{\sinh\left(u_j - \frac{i\gamma}{2}\right)} \right]^{2N+2} \left[\frac{\cosh\left(u_j - \frac{i\gamma}{2}\right)}{\cosh\left(u_j + \frac{i\gamma}{2}\right)} \right]^2$$

$$= \prod_{\sigma=\pm 1} \prod_{k\neq j}^{M} \frac{\sinh(u_j + \sigma u_k + i\gamma)}{\sinh(u_j + \sigma u_k - i\gamma)}, \quad j = 1, \ldots, M. \tag{34}$$

The energy levels of the coherent model in Eqs. (27) and (32) and of the dissipative constrained model E_α, $\nu_\alpha \propto \exp(-\tilde{E}_\alpha)$, are given by the usual $E_\alpha = (N+1)\Delta + \sum_{j=1}^M \epsilon(u_{j,\alpha})$,

$\tilde{E}_\alpha = \sum_{j=1}^{M} \tilde{\epsilon}(u_{j,\alpha})$, with original and dissipatively dressed dispersions

$$\epsilon(u) = \frac{-2\sin^2\gamma}{\sinh\left(u+\frac{i\gamma}{2}\right)\sinh\left(u-\frac{i\gamma}{2}\right)}, \tag{35}$$

$$\tilde{\epsilon}(u) = 2\ln\left|\frac{\cosh\left(u+\frac{i\gamma}{2}\right)\cosh\left(u-\frac{i\gamma}{2}\right)}{\sinh\left(u+\frac{i\gamma}{2}\right)\sinh\left(u-\frac{i\gamma}{2}\right)}\right| = 2\ln\left|\frac{\Delta\,\epsilon(v)}{2(1-\Delta^2)}-1\right|. \tag{36}$$

Note that the original dispersion $\epsilon(u)$ is the same as in the $U(1)$ invariant XXZ case even though the nature of the eigenstates $|\alpha\rangle$ is here completely different. Note also that after a standard substitution $e^{ip} = \frac{\sinh(u+\frac{i\gamma}{2})}{\sinh(u-\frac{i\gamma}{2})}$ the dispersion relation $\epsilon(u)$ acquires a more familiar form: $\epsilon(p) = 4(\cos p - \Delta)$.

All eigenstates within G_M are chiral, since they are a linear superposition of spin helix pieces with the same helicity [Eq. (36)]. The "chiral quasiparticles" do not carry fixed magnetization as in the $U(1)$ case [Eq. (27)], but rather form domain walls, or kinks, on top of a chiral "background" (see Ref. [18] for more details). Equation (36) is proved in Sec. V, while its generalization for $M > 1$ is a conjecture based on numerics (see Appendix B).

XYZ model with chiral invariant subspace. Finally we consider a fully anisotropic XYZ spin chain

$$H_D = \sum_{n=1}^{N-1} \vec{\sigma}_n \cdot \hat{J}\vec{\sigma}_{n+1} + h_1(\vec{n}_l) + h_N(\vec{n}_r),$$
$$\hat{J} = \mathrm{diag}(J_x,\, J_y,\, J_z), \tag{37}$$

where h_1 and h_N are given by Eqs. (10) and (11). J_α can be parametrized in terms of two complex parameters η, τ and the Jacobi θ functions as $\{J_x, J_y, J_z\} = \{\frac{\theta_4(\eta)}{\theta_4(0)}, \frac{\theta_3(\eta)}{\theta_3(0)}, \frac{\theta_2(\eta)}{\theta_2(0)}\}$. Following Ref. [19], we use the shorthand notation $\theta_\alpha(u) \equiv \vartheta_\alpha(\pi u|e^{i\pi\tau})$, $\tilde{\theta}_\alpha(u) \equiv \vartheta_\alpha(\pi u|e^{2i\pi\tau})$. Real η and purely imaginary τ with $\mathrm{Im}(\tau) > 0$ give real J_α.

As explained in Sec. II, Eq. (37) describes an effective dynamics (13) for an XYZ spin chain with boundary spins dissipatively projected onto fully polarized states $\vec{n}_l, \vec{n}_r$. If is convenient to parametrize unit vectors $\vec{n}_l, \vec{n}_r$ by two complex parameters $u_l = x_l + iy_l$ and $u_r = x_r + iy_r$ as [20]

$$n^x_{l,r} = -\frac{\theta_2(iy_{l,r})}{\theta_3(iy_{l,r})}\frac{\theta_1(x_{l,r})}{\theta_4(x_{l,r})},$$
$$n^y_{l,r} = -i\frac{\theta_1(iy_{l,r})}{\theta_3(iy_{l,r})}\frac{\theta_2(x_{l,r})}{\theta_4(x_{l,r})},$$
$$n^z_{l,r} = -\frac{\theta_4(iy_{l,r})}{\theta_3(iy_{l,r})}\frac{\theta_3(x_{l,r})}{\theta_4(x_{l,r})}. \tag{38}$$

We focus on eigenstates of Eqs. (37) within a chiral invariant subspace G_M with dimension $\binom{N+1}{M}$, which appears for $x_r = x_l + (N+1-2M)\eta$, $y_r = y_l$, and integer $M \in [0, N+1]$ [20]. This chiral subspace is an elliptic extension of the spin-helix-based chiral subspace in the previous example. Each state $|\alpha\rangle$ within the invariant subspace is parametrized via M Bethe rapidities $\{u_{j,\alpha}\}$, which satisfy the following BAE [21] (see also Appendix C):

$$\left[\frac{\theta_1\left(u_j+\frac{\eta}{2}\right)}{\theta_1\left(u_j-\frac{\eta}{2}\right)}\right]^{2N+2}\frac{\theta_3\left(u_j+iy_l-\frac{\eta}{2}\right)}{\theta_3\left(u_j-iy_l+\frac{\eta}{2}\right)}\frac{\theta_4\left(u_j+x_l-\frac{\eta}{2}\right)}{\theta_4\left(u_j-x_l+\frac{\eta}{2}\right)} \times \frac{\theta_3\left(u_j-iy_r-\frac{\eta}{2}\right)}{\theta_3\left(u_j+iy_r+\frac{\eta}{2}\right)}\frac{\theta_4\left(u_j-x_r-\frac{\eta}{2}\right)}{\theta_4\left(u_j+x_r+\frac{\eta}{2}\right)} = \prod_{\sigma=\pm1}\prod_{k\neq j}^{M}\frac{\theta_1(u_j+\sigma u_k+\eta)}{\theta_1(u_j+\sigma u_k-\eta)}, \quad j=1,\ldots,M. \tag{39}$$

The energy of the model can be expressed in terms of Bethe rapidities $\{u_{j,\alpha}\}$ as

$$E_\alpha = \sum_{j=1}^{M}\epsilon(u_{j,\alpha}) + (N+1)g(\eta) + g\left(\frac{\tau}{2}+x_l\right) - g\left(\frac{\tau}{2}+x_r\right), \tag{40}$$

$$g(u) = \frac{\theta_1(\eta)\theta_1'(u)}{\theta_1'(0)\theta_1(u)}, \quad \theta_1'(u) = \frac{\partial\theta_1(u)}{\partial u}, \tag{41}$$

where $\epsilon(u)$ is the original dispersion relation

$$\epsilon(u) = 2\left[g\left(u-\frac{\eta}{2}\right) - g\left(u+\frac{\eta}{2}\right)\right]. \tag{42}$$

On the basis of numerical studies (see Appendix D), we conjecture that the dissipative dressing effect takes place also here, i.e., $\rho_{\mathrm{NESS}} = \tilde{Z}^{-1}\sum_\alpha \exp(-\tilde{E}_\alpha)|\alpha\rangle\langle\alpha|$ with $\tilde{E}_\alpha = \sum_{j=1}^{M}\tilde{\epsilon}(u_{j,\alpha})$, where

$$\tilde{\epsilon}(u) = 2\ln\left|\frac{Q\left(\frac{1-\tau}{2}+i\,\mathrm{Im}\,u_l, u\right)}{Q(0,u)}\right|,$$
$$Q(x,u) = \theta_1\left(x-u+\frac{\eta}{2}\right)\theta_1\left(x+u+\frac{\eta}{2}\right). \tag{43}$$

By letting $i\,\mathrm{Im}\,u_l = \tau/2$ and $\tau \to +i\infty$, one recovers from Eqs. (43) the XXZ limit (36) with $\gamma = \pi\eta$. More details are given in Appendix D.

IV. *XXX/XXZ* MODEL WITH SINK AND SOURCE: DERIVATION OF DISSIPATIVE DRESSING RELATIONS

The derivation of the expressions for dissipatively dressed dispersion appears rather technical, as any problem having to do with finding correlation functions of interacting many-body systems would. Here we show how to derive the simplest of our results, Eq. (26), for the dissipatively dressed dispersion of an isotropic Heisenberg model with sink and source, in a pedagogical way.

The eigenstates of

$$H_D = \sum_{n=1}^{N-1}\vec{\sigma}_n\cdot\vec{\sigma}_{n+1} - \sigma_1^z + \sigma_N^z \tag{44}$$

can be separated into blocks with fixed total magnetization due to $U(1)$ symmetry. Since ρ_{NESS} commutes with Eq. (44), H and ρ_{NESS} can be diagonalized simultaneously. The simplest eigenstate of H is a state with maximal possible

magnetization $|0\rangle \equiv |\uparrow\uparrow\cdots\uparrow\rangle$. In the block with $M = 1, 2, \ldots$ spins down, the eigenstates have the form

$$|\alpha\rangle = \sum_{n=1}^{N} \gamma_n(u_\alpha)\, \sigma_n^- |0\rangle, \tag{45}$$

$$|\beta\rangle = \sum_{n_1,n_2=1}^{N} \gamma_{n_1,n_2}(u_{1,\beta}, u_{2,\beta})\, \sigma_{n_1}^- \sigma_{n_2}^- |0\rangle, \ldots. \tag{46}$$

Assuming nondegeneracy of the spectrum of H, $\rho_{\rm NESS}$ has the same eigenstates and can be written as

$$\rho_{\rm NESS} = \nu_0 |0\rangle\langle 0| + \sum_{\alpha=1}^{N} \nu_\alpha^{(1)} |\alpha\rangle\langle\alpha| + \cdots, \tag{47}$$

where $\cdots$ denotes contributions from blocks with $M > 1$. From Eqs. (14) and (15), we find $g_l = \sigma_1^-$ and $g_r = \sigma_N^+$.

According to detailed balance relations (21) (that can be proved *a posteriori*), $\nu_\alpha^{(1)}/\nu_0 = w_{0\alpha}/w_{\alpha 0}$. From Eq. (18) we find

$$\frac{w_{0\alpha}}{w_{\alpha 0}} = \frac{|\langle\alpha|\sigma_1^-|0\rangle|^2 + |\langle\alpha|\sigma_N^+|0\rangle|^2}{|\langle 0|\sigma_1^-|\alpha\rangle|^2 + |\langle 0|\sigma_N^+|\alpha\rangle|^2} = \frac{|\langle\alpha|\sigma_1^-|0\rangle|^2}{|\langle 0|\sigma_N^+|\alpha\rangle|^2} = \left|\frac{\gamma_1}{\gamma_N}\right|^2. \tag{48}$$

In order to find the ratio γ_1/γ_N, we use the algebraic Bethe Ansatz method. Within the method, the eigenvectors of H are produced by repetitive action of a "creation" operator $\mathbb{B}(u)$ on the vacuum state $|0\rangle$. Each application of $\mathbb{B}(u)$ lowers the total magnetization by 1, so, e.g., eigenstates from Eqs. (45) and (46) are produced as $|\alpha\rangle = \mathbb{B}(u_{1,\alpha})|0\rangle$, $|\beta\rangle = \mathbb{B}(u_{1,\beta})\mathbb{B}(u_{2,\beta})|0\rangle$. Here $u_{j,\alpha}, u_{j,\beta}$ are Bethe roots [solutions of Eq. (23)] for $M = 1$ and $M = 2$, respectively.

Let us first introduce the double-row monodromy matrix,

$$\mathcal{T}_0(u) = T_0(u)\mathcal{K}_0(u)\bar{T}_0(u), \tag{49}$$

where subscript 0 denotes the two-dimensional auxiliary space. The one-row monodromy matrices $T(u)$, $\bar{T}(u)$ and the K matrix in Eq. (49) are defined as

$$T(u) = R_{0,N}(u)\cdots R_{0,1}(u) = \begin{pmatrix} A(u) & B(u) \\ C(u) & D(u) \end{pmatrix}, \tag{50}$$

$$\bar{T}(u) = R_{0,1}(u)\cdots R_{0,N}(u) = \begin{pmatrix} \bar{A}(u) & \bar{B}(u) \\ \bar{C}(u) & \bar{D}(u) \end{pmatrix}, \tag{51}$$

$$R_{0,n}(u) = \begin{pmatrix} uI + \frac{i}{2}\sigma_n^z & i\sigma_n^- \\ i\sigma_n^+ & uI - \frac{i}{2}\sigma_n^z \end{pmatrix}, \tag{52}$$

and

$$\mathcal{K}(u) = \mathrm{diag}\{u^{[-3]}, \ -u^{[1]}\}. \tag{53}$$

The "eigenstates" creation operator $\mathbb{B}(u)$ is an element of $\mathcal{T}(u)$:

$$\mathbb{B}(u) = [\mathcal{T}(u)]_2^1 = u^{[-3]}A(u)\bar{B}(u) - u^{[1]}B(u)\bar{D}(u). \tag{54}$$

The following relation,

$$T_1(u)R_{1,2}\left(2u - \frac{i}{2}\right)\bar{T}_2(u) = \bar{T}_2(u)R_{1,2}\left(2u - \frac{i}{2}\right)T_1(u), \tag{55}$$

leads to

$$A(u)\bar{B}(u) = \frac{2u - i}{2u}\bar{B}(u)A(u) - \frac{i}{2u}B(u)\bar{D}(u). \tag{56}$$

Then, we derive

$$\mathbb{B}(u) = \frac{u^{[-3]}u^{[-1]}}{u}\bar{B}(u)A(u) - \frac{u^{[3]}u^{[-1]}}{u}B(u)\bar{D}(u). \tag{57}$$

From the explicit form of the one-row monodromy matrices, we obtain

$$A(u)|0\rangle = (u^{[1]})^N|0\rangle, \tag{58}$$

$$\bar{D}(u)|0\rangle = (u^{[-1]})^N|0\rangle, \tag{59}$$

$$\bar{B}(u)|0\rangle = i\sum_{m=1}^{N} F_m(u)\,\sigma_m^-|0\rangle, \tag{60}$$

$$B(u)|0\rangle = i\sum_{m=1}^{N} F_{N-m+1}(u)\sigma_m^-|0\rangle, \tag{61}$$

$$F_m(u) = (u^{[1]})^{m-1}(u^{[-1]})^{N-m}. \tag{62}$$

The Bethe state $\mathbb{B}(u)|0\rangle$ can be expanded as

$$\mathbb{B}(u)|0\rangle = i\frac{u^{[-3]}u^{[-1]}}{u}(u^{[1]})^N\sum_{m=1}^{N}F_m(u)\,\sigma_m^-|0\rangle - i\frac{u^{[3]}u^{[-1]}}{u}(u^{[-1]})^N\sum_{m=1}^{N}F_{N-m+1}(u)\sigma_m^-|0\rangle. \tag{63}$$

With the help of Eq. (63), it can be derived that

$$\gamma_1(u) = 2(u^{[-1]})^N(u^{[1]})^{N-1}, \tag{64}$$

$$\gamma_N(u) = \frac{iu^{[-3]}u^{[-1]}(u^{[1]})^{2N-1} - iu^{[3]}(u^{[-1]})^{2N}}{u} \overset{(23)}{=} 2(u^{[-1]})^{2N}u^{[3]}(u^{[1]})^{-2}. \tag{65}$$

One can thus obtain the ratio

$$\frac{\gamma_1^2(u)}{\gamma_N^2(u)} = \left(\frac{u^{[1]}}{u^{[-1]}}\right)^{2N}\left(\frac{u^{[1]}}{u^{[3]}}\right)^2 \overset{(23)}{=} \frac{u^{[1]}u^{[-1]}}{u^{[3]}u^{[-3]}}, \tag{66}$$

leading to Eq. (26) for $M = 1$.

Proceeding iteratively for $M = 2, 3, \ldots$, one can verify the general validity of Eq. (26). In Ref. [6] we prove Eq. (26) via an alternative method.

The effects of a dissipative dressing on the NESS spectrum can be seen already in the one-particle sector $M = 1$. Notably, the bare (original) quasiparticle dispersion $\epsilon(u)$ has a singularity at $u = \pm i/2$, while the dissipatively dressed quasiparticle dispersion $\tilde{\epsilon}(u)$ [Eq. (66)] retains the singularity at $u = \pm i/2$ and acquires an extra singularity at $u = \pm 3i/2$. In the following we show that some solutions of the BAE lie exponentially close to the extra singularity $u = \pm 3i/2$, drastically modifying the NESS spectrum $\tilde{E}_\alpha$ with respect to the H spectrum E_α.

The sector $M = 1$ contains N Bethe eigenstates $|\alpha\rangle$ parametrized by the solutions u_α, $\alpha = 1, \ldots, N$, of BAE (23). Among the N BAE solutions there are always $N - 1$ real solutions, say, $u_2, \ldots, u_N$, and one boundary localized imaginary solution u_1, lying exponentially close to the extra singularity due to dissipative dressing, namely, $u_1 = i(3/2 + O(2^{-N}))$ (see the top panel of Fig. 2). Explicitly, from Eq. (23) we

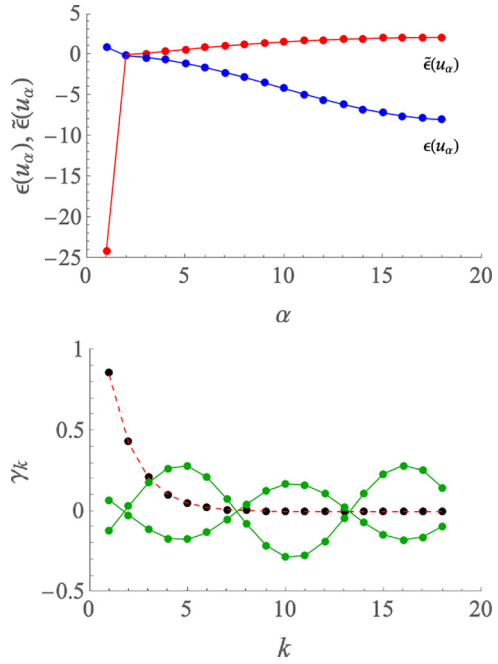

FIG. 2. Top: quasiparticle energies $\epsilon(u_\alpha)$ (blue joined points) and their dissipative dressing $\tilde{\epsilon}(u_\alpha)$ (red joined points) in the *XXX* model with $N = 18$ spin, in the block with one magnon $M = 1$. The state $\alpha = 1$ is a localized Bethe state with $u_1 \simeq 3i/2 + ie^{-24.5}$. Bottom: coefficients γ_k of the normalized localized Bethe state $|\alpha = 1\rangle = \sum_{k=1}^{N} \gamma_k \sigma_k^- |0\rangle$ (open black circles). The dashed red line is the fit $\gamma_k = 1.7 \times 2^{-k}$. The green joined points are the coefficients Re γ_k and Im γ_k for the plane-wave-like Bethe state with $u_4 \approx 1.78139$.

find $u_1 - 3i/2 \equiv \delta = 3i2^{-2N-1}(1 + O(N\delta))$. The corresponding dressed energy $\tilde{\epsilon}(u_1)$ is drastically renormalized by the singularity, acquiring a negative amplitude linearly growing with system size, $\tilde{\epsilon}(u_1) \approx -2(N+1)\ln 2 + \ln 9$ [see Eq. (79)]. On the other hand, for plane-wave-type (real u_j) BAE solutions, the dressed and original energies are comparable. As a result, $e^{-\tilde{\epsilon}(u_1)} \gg e^{-\tilde{\epsilon}(u_\alpha)}$ for $\alpha > 1$, and in the NESS, the boundary localized Bethe eigenstate $|\alpha = 1\rangle$ comes with an exponentially large (in system size N) relative weight in sum (3) with respect to the plane-wave $M = 1$ eigenstates $|\alpha\rangle$ (see Fig. 2). In sectors with several quasiparticles $M > 1$ we observe a similar phenomenon, which leads to an overall subextensive scaling of the von Neumann entropy of the NESS [Eq. (3)] with the system size (see Ref. [6]).

Trigonometric case. We pass to the trigonometric *XXZ* case [Eq. (27)] by redefining the functions $u^{[k]}$ as Eq. (29). The dispersion relation of the quasiparticles has the form

$$\epsilon(u) = -\frac{2\sin^2\gamma}{u^{[1]}u^{[-1]}}, \tag{67}$$

and the *XXZ* eigenvalues are

$$E = \sum_{j=1}^{M} \epsilon(u_j) + (N-1)\cos\gamma, \tag{68}$$

where $\{u_j\}$ are solutions of BAE (23), with redefinition (29). The one-particle wave function is given by expression (63) with the replacements (29) and $i \to i\sin\gamma$.

Repeating the calculations, we find

$$\frac{v_\alpha^{(1)}}{v_0} = \frac{u^{[1]}u^{[-1]}}{u^{[3]}u^{[-3]}}, \tag{69}$$

leading to Eq. (31) for $M = 1$.

Proceeding analogously for $M = 2, 3, \ldots$, one can verify the validity of Eq. (31) and, consequently, of Eq. (26), iteratively. In Ref. [6] we obtain the result, Eq. (31), in an alternative way, expressing the operators g_l, g_r in terms of $\mathbb{B}(u)$ and using the commutation relation between the monodromy matrix elements.

Let us analyze the BAE solutions for the $M = 1$ case in more detail. The corresponding Bethe states can be rewritten in terms of the quasimomentum p as

$$\sum_{n=1}^{N} \mathcal{A}_n(p)\,\sigma_n^- |0\rangle, \tag{70}$$

$$\mathcal{A}_n(p) = (e^{ip} - 2\Delta)e^{inp} - (1 - 2\Delta e^{ip})e^{i(1-n)p}, \tag{71}$$

where p satisfies

$$e^{i(2N+1)p}(e^{ip} - 2\Delta) - (1 - 2\Delta e^{ip}) = 0. \tag{72}$$

Most solutions for p of Eq. (72) are real. However, in some cases, Eq. (72) has an imaginary solution. Indeed, let us define a function

$$\mathcal{W}(x) = x^{(2N+1)}(x - 2\Delta) - (1 - 2\Delta x). \tag{73}$$

One can easily check that

$$\mathcal{W}(1) = 0, \quad \mathcal{W}\left(\frac{1}{2\Delta}\right) = (1 - 4\Delta^2)(2\Delta)^{-2N-2},$$
$$\mathcal{W}(2\Delta) = 4\Delta^2 - 1, \quad \mathcal{W}'(1) = 2 + 2N(1 - 2\Delta). \tag{74}$$

Once

$$\Delta > \frac{1}{2}, \quad N > \frac{1}{2\Delta - 1}, \tag{75}$$

we have

$$\mathcal{W}\left(\frac{1}{2\Delta}\right) < 0, \quad \mathcal{W}(1) = 0, \quad \mathcal{W}'(1) < 0. \tag{76}$$

Therefore, $\mathcal{W}(x) = 0$ has a solution in the interval $(\frac{1}{2\Delta}, 1)$ under condition (75). And, from Eq. (73), the root approaches $\frac{1}{2\Delta}$ as N increases. Since $\mathcal{W}(e^{ip}) = 0$ is exactly BAE (72), this implies an imaginary root p with $e^{ip} \approx \frac{1}{2\Delta}$ (or, equivalently, $u \approx -\frac{3i\gamma}{2}$). When N is large enough, this imaginary p will give a localized state with

$$\mathcal{A}_n(p) \approx \left(\frac{1}{2\Delta} - 2\Delta\right)\left(\frac{1}{2\Delta}\right)^n. \tag{77}$$

The dressed energy in terms of p is

$$\ln|e^{-ip}(e^{ip} - 2\Delta)(1 - 2\Delta e^{ip})| \overset{(72)}{=} \ln|e^{2iNp}(e^{ip} - 2\Delta)^2|. \tag{78}$$

For the imaginary solution $e^{ip} \approx \frac{1}{2\Delta}$ for large N, the dressed energy $\tilde{\epsilon}(p)$ becomes

$$\tilde{\epsilon} \approx \ln|(2\Delta)^{-2N-2}(1 - 4\Delta^2)^2|$$
$$= -2(N+1)\ln(2\Delta) + 2\ln(4\Delta^2 - 1).$$

In particular, for $\Delta = 1$ we obtain

$$\tilde{\epsilon} \approx -2(N+1)\ln 2 + \ln 9. \tag{79}$$

V. *XXZ* MODEL WITH CHIRAL INVARIANT SUBSPACE: DERIVATION OF DISSIPATIVELY DRESSED DISPERSION [EQ. (36)]

Like in the previous section, we first prove Eq. (36) for the single-quasiparticle $M = 1$ sector.

Let us introduce the following family of chiral states:

$$\begin{aligned}\langle \Phi(n_1,\dots,n_M)| = \exp\left[i\gamma\sum_k n_k\right]\bigotimes_{l_1=1}^{n_1}\phi(l_1)\\ \bigotimes_{l_2=n_1+1}^{n_2}\phi(l_2-2)\cdots\\ \bigotimes_{l_{M+1}=n_M+1}^{N}\phi(l_{M+1}-2M),\end{aligned}$$

$$\phi(n) = \frac{1}{\sqrt{2}}(1,\ e^{-in\gamma}). \tag{80}$$

Then, the set

$$\langle \Phi(n_1,\dots,n_M)|, \quad 0 \leqslant n_1 < n_2 \cdots < n_M \leqslant N,$$

forms an invariant subspace of the Hamiltonians (27) and (32) [16]. A chiral analog of the coordinate Bethe Ansatz [18] then leads to the consistency conditions which have the form of standard BAE (34). We aim at finding NESS eigenvalues, corresponding to the invariant subspace eigenstates $|\alpha\rangle$ of Eqs. (27) and (32). According to Eq. (21), the ratio of the NESS eigenvalues for the associated dissipative problem (Fig. 1) is given by

$$\frac{\nu_\alpha}{\nu_\beta} = \frac{w_{\beta\alpha}}{w_{\alpha\beta}} = \frac{|\langle\alpha|g_l|\beta\rangle|^2 + |\langle\alpha|g_r|0\rangle|^2}{|\langle\beta|g_l|\alpha\rangle|^2 + |\langle\beta|g_r|\alpha\rangle|^2}, \tag{81}$$

with operators $g_{l,r}$ computed from Eqs. (14) and (15):

$$\begin{aligned} g_l &= G_L \otimes I^{\otimes_{N-1}}, \quad g_r = I^{\otimes_{N-1}} \otimes G_R,\\ G_{L,R} &= \begin{pmatrix} \cos\gamma & -e^{-i\varphi_{l,r}} \\ e^{i\varphi_{l,r}} & -\cos\gamma \end{pmatrix},\\ \varphi_l &= 0,\ \ \varphi_r = \varphi(M). \end{aligned} \tag{82}$$

Let us calculate Eq. (81) for $M = 1$, where the Bethe states have the form [16]

$$\langle\alpha| = \sum_{n=0}^{N}\langle\Phi(n)|f_n(p^{(\alpha)}), \tag{83}$$

$$f_n(p) = e^{i\chi+inp} + e^{-i\chi-inp}, \quad e^{2i\chi(p)} = \frac{\Delta - e^{ip}}{e^{-ip}-\Delta}. \tag{84}$$

Here, the "quasimomentum" p and the rapidity u from Eq. (34) are related by standard relation

$$e^{ip} = \frac{\sinh\left(u+\frac{i\gamma}{2}\right)}{\sinh\left(u-\frac{i\gamma}{2}\right)}. \tag{85}$$

In terms of p, BAE (34) for $M = 1$ acquires a simple form,

$$e^{2iNp}e^{4i\chi} = 1. \tag{86}$$

All solutions p_α of Eq. (86) are real, meaning that also $f_n(p_\alpha)$ are all real.

To compute the expressions $\langle\alpha|g_l|\beta\rangle$ in Eq. (81) we note the following property:

$$\begin{aligned} g_l|\Phi(n)\rangle &= \kappa(2\delta_{n,0}-1)|\Phi(n)\rangle,\\ g_r|\Phi(n)\rangle &= \kappa(1-2\delta_{n,N})|\Phi(n)\rangle,\\ \kappa &= i\sin\gamma. \end{aligned} \tag{87}$$

While the eigenstates $|\alpha\rangle$ in Eq. (83) are orthonormal, the chiral states $|\Phi(n)\rangle$ are not:

$$\langle\Phi(n)|\Phi(m)\rangle = \Delta^{|n-m|}. \tag{88}$$

For further calculations we set

$$p \equiv p_\alpha,\ p' \equiv p_\beta, \quad \chi \equiv \chi(p_\alpha),\ \chi' \equiv \chi(p_\beta), \tag{89}$$

for notational simplicity. Using Eqs. (87) and (88), $\langle\alpha|\beta\rangle = 0$, and $f_n^* = f_n$, we obtain

$$\langle\alpha|g_l|\beta\rangle = 2\kappa f_0(p')\sum_{n=0}^{N} f_n(p)\Delta^n, \tag{90}$$

$$\langle\alpha|g_r|\beta\rangle = -2\kappa f_N(p')\sum_{n=0}^{N} f_{N-n}(p)\Delta^n. \tag{91}$$

From Eq. (86), we readily find

$$f_{N-n}(p) = \pm f_n(p). \tag{92}$$

It follows that

$$|\langle\alpha|g_l|\beta\rangle| = |\langle\alpha|g_r|\beta\rangle|, \tag{93}$$

and consequently

$$\frac{\nu_\alpha}{\nu_\beta} = \frac{|\langle\alpha|g_l|\beta\rangle|^2}{|\langle\beta|g_l|\alpha\rangle|^2}. \tag{94}$$

Performing summation in Eq. (90), we obtain

$$\begin{aligned}\langle\alpha|g_l|\beta\rangle &= 2\kappa f_0(p')\sum_{n=0}^{N} f_n(p)\Delta^n\\ &= 2\kappa f_0(p')\left(e^{i\chi}\frac{1-z_+^{N+1}}{1-z_+} + e^{-i\chi}\frac{1-z_-^{N+1}}{1-z_-}\right),\\ z_\pm &= e^{\pm ip}\Delta.\end{aligned}$$

Remarkably, due to BAE (86), the N dependence in the above vanishes:

$$\begin{aligned} &e^{i\chi}\frac{z_+^{N+1}}{1-z_+} + e^{-i\chi}\frac{z_-^{N+1}}{1-z_-}\\ &= z_-^{N+1}e^{-i\chi}\left(\frac{e^{2iNp+2i\chi}e^{2ip}}{1-z_+} + \frac{1}{1-z_-}\right)\\ &= z_-^{N+1}e^{-i\chi}\left(\frac{e^{-2i\chi}e^{2ip}}{1-z_+} + \frac{1}{1-z_-}\right)\\ &= z_-^{N+1}e^{-i\chi}\left(e^{-ip}\frac{1-z_+}{\Delta-e^{ip}}\frac{e^{2ip}}{1-z_+} + \frac{1}{1-z_-}\right)\\ &= 0. \end{aligned} \tag{95}$$

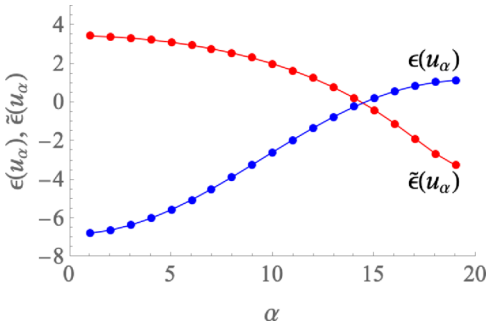

FIG. 3. Quasiparticle energies $\epsilon(u_\alpha)$ (blue joined points) and dissipatively dressed ones $\tilde{\epsilon}(u_\alpha)$ (red joined points) in the *XXZ* model with chiral invariant subspace, in the block with one kink, $M = 1$. Parameters: $N = 18$, $\Delta = 0.7$. There are no localized states: all the amplitudes are plane-wave-like; data not shown.

So we obtain

$$\frac{\langle\alpha|g_l|\beta\rangle}{2\kappa} = f_0(p')\left(\frac{e^{i\chi}}{1-z_+} + \frac{e^{-i\chi}}{1-z_-}\right). \tag{96}$$

From Eq. (84) we have

$$e^{i\chi}(e^{-ip} - \Delta) = e^{-i\chi}(\Delta - e^{ip}),$$

and for the real part

$$\cos(\chi - p) = \Delta\cos\chi. \tag{97}$$

Noting $f_0(p') = 2\cos\chi'$ and using Eq. (97), after some straightforward algebra we obtain

$$\langle\alpha|g_l|\beta\rangle = \frac{8\kappa(\Delta^{-1} - \Delta)\cos\chi'\cos\chi}{\Delta + \Delta^{-1} - 2\cos p}. \tag{98}$$

The expression for $\langle\beta|g_l|\alpha\rangle$ is obtained from the above by substitutions $p \leftrightarrow p'$, $\chi \leftrightarrow \chi'$, yielding

$$\frac{\langle\alpha|g_l|\beta\rangle}{\langle\beta|g_l|\alpha\rangle} = \frac{\Delta + \Delta^{-1} - 2\cos p'}{\Delta + \Delta^{-1} - 2\cos p}. \tag{99}$$

Notably, the Kolmogorov relation [Eq. (20)] follows from Eq. (99), justifying *a posteriori* the assumption (81).

Restoring the original notations (89) we get

$$\frac{\nu_\alpha}{\nu_\beta} = \frac{|\Delta + \Delta^{-1} - 2\cos p_\beta|^2}{|\Delta + \Delta^{-1} - 2\cos p_\alpha|^2}. \tag{100}$$

Finally, using $\ln\frac{\nu_\beta}{\nu_\alpha} = \tilde{E}_\alpha - \tilde{E}_\beta = \tilde{\epsilon}(u_\alpha) - \tilde{\epsilon}(u_\beta)$, and Eq. (85), Eq. (100) reduces to Eq. (36).

Figure 3 shows dissipatively dressed and original energies for the multiplet from chiral invariant subspace with $M = 1$. We see that the dissipative dressing reverses the order of the contributions in the respective NESS with respect to the Gibbs state (for $\epsilon(u_\alpha) < \epsilon(u_\beta)$, $\tilde{\epsilon}(u_\alpha) > \tilde{\epsilon}(u_\beta)$). However, unlike in the *XXZ* model with diagonal boundary fields, we do not see drastic renormalization effects for some eigenstates like in Fig. 2. This happens because all Bethe roots u_j are now real, and therefore cannot approach singularities of $\tilde{\epsilon}(u)$, lying on the imaginary axis, as it happened in the "sink and source" case (Fig. 2).

Even though there are no principal difficulties to extend the above calculations for larger M using the chiral Bethe Ansatz method [18], the analytic expressions become difficult to handle because of the nonorthogonality of the chiral basis vectors (80). For $M > 1$ the validity of Eq. (36) is thus checked numerically (see Appendix B).

VI. DISCUSSION

In summary, we have found and described a surprising effect of dissipative dressing of a quasiparticle dispersion relation, in integrable spin chains attached to strongly dissipative baths. So far we have been able to find a rigorous proof only for the $U(1)$-symmetric "sink and source" case [Eq. (31)], which is valid for all eigenstates (see the companion paper [6]). However, the effect of dissipative dressing is definitely present in other integrable systems as discussed in the present paper, including the fully anisotropic *XYZ* model, as suggested by firm numerical evidence. For all the cases, we find the dissipatively dressed dispersion relation (energy of quasiparticle) of the form

$$\tilde{\epsilon}(u) \sim \ln(\epsilon(u)/f(u)), \tag{101}$$

where u is a Bethe rapidity, $\epsilon(u)$ is the original quasiparticle dispersion, and $f(u)$ contains an additional singularity. While for the *XXZ* model the property (101) is obvious by comparison of Eqs. (31) and (36) with Eq. (35), for the *XYZ* model, Eq. (101) seems not obviously true. However, also for the *XYZ* case, our numerical data confirm the validity of Eq. (101), where $f(u)$ depends on extra complex parameters (to be reported elsewhere).

Using the dissipatively dressed dispersion relation as a key input we have been able to diagonalize the steady-state density operators of boundary dissipatively driven integrable quantum spin chains in the limit of large dissipation, also known as the Zeno regime, by employing the Bethe Ansatz of a related dissipation-projected Hamiltonian. We have thus discovered a simple but surprising phenomenon of "dissipative dressing" of quasiparticle energies in integrable coherent systems exposed to boundary dissipation.

Our results should have applications in state engineering and dissipative state preparation. Moreover, we expect analogous emergent integrability of the steady-state density operators in the discrete-time case of integrable Floquet *XXX*, *XXZ*, and *XYZ* circuits, where boundary dissipation can be conveniently implemented by the so-called reset channel [12,22].

ACKNOWLEDGMENTS

V.P. and T.P. acknowledge support by ERC Advanced Grant No. 101096208 – QUEST, and Research Program P1-0402 and Grant No. N1-0368 of the Slovenian Research and Innovation Agency (ARIS). V.P. is also supported by Deutsche Forschungsgemeinschaft through DFG Project No. KL645/20-2. X.Z. acknowledges financial support from the National Natural Science Foundation of China (Grant No. 12204519).

DATA AVAILABILITY

No data were created or analyzed in this study.

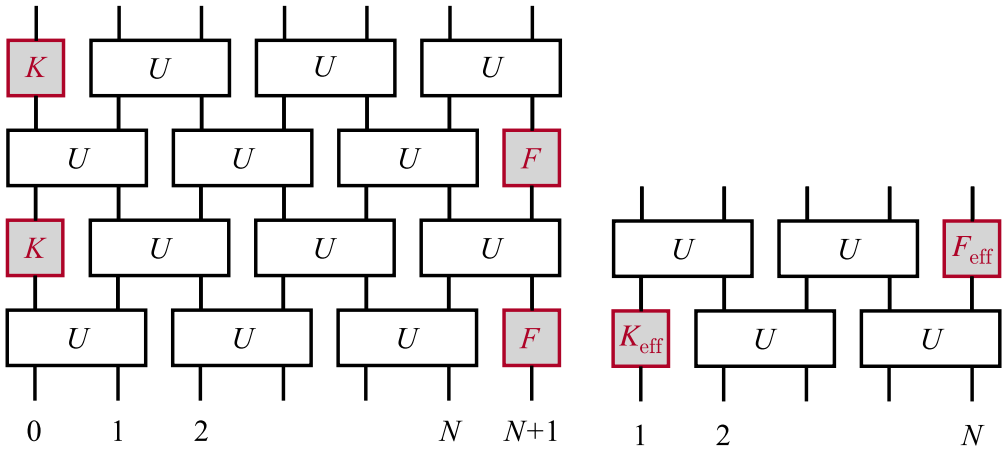

FIG. 4. Brick-wall unitary circuit (BUC), original (left) and effective (right). Left: Original BUC with reset gates K and F at the edges. Two-body interaction U is given by Eq. (A4). Right: Effective BUC, where the first site and the last site are traced out, giving rise to effective Krauss operators $K_{\rm eff}$ and $F_{\rm eff}$.

APPENDIX A: LINDBLAD MASTER EQUATION EVOLUTION AS A LIMIT OF A BRICK-WALL UNITARY CIRCUIT

Here we describe a brick-wall unitary circuit leading to the Lindblad Master equation [Eq. (7)] with an *XXX* Hamiltonian in the continuous-time (Trotter) limit.

It is described by a two-step discrete-time protocol, schematically shown in Fig. 4. Assuming N being odd, the discrete evolution has the following form:

$$\mathcal{M} = \mathcal{M}_{\rm odd}\mathcal{M}_{\rm even}, \tag{A1}$$

$$\mathcal{M}_{\rm even}[\rho] = \sum_{j=1}^{2} F_j(\epsilon) U_{01}U_{23}\cdots U_{N-1,N}\ \rho\ U_{01}^\dagger \times U_{23}^\dagger\cdots U_{N-1,N}^\dagger F_j(\epsilon)^\dagger, \tag{A2}$$

$$\mathcal{M}_{\rm odd}[\rho] = \sum_{j=1}^{2} K_j(\epsilon) U_{12}U_{34}\cdots U_{N,N+1}\ \rho\ U_{12}^\dagger \times U_{34}^\dagger\cdots U_{N,N+1}^\dagger K_j(\epsilon)^\dagger, \tag{A3}$$

$$U_{n,n+1} = \frac{1-i\tau P_{n,n+1}}{1-i\tau},$$

$$P_{n,n+1} = \frac{1}{2}(I + \vec{\sigma}_n\cdot\vec{\sigma}_{n+1}), \tag{A4}$$

where $P_{n,n+1}$ is a permutation, τ is a real number, and the Krauss gates $K_j(\epsilon)$, $F_j(\epsilon)$, $0 \leqslant \epsilon < 1$, act on spins 0 and $N+1$, respectively (see Fig. 4). Explicitly the Krauss gates are given by

$$F_1(\epsilon) = \sqrt{1-\epsilon}\ \sigma^+_{N+1}, \quad F_2(\epsilon) = \begin{pmatrix} 1 & 0 \\ 0 & \sqrt{\epsilon} \end{pmatrix}, \tag{A5}$$

$$K_1(\epsilon) = \sqrt{1-\epsilon}\,\sigma^-_0, \quad K_2(\epsilon) = \begin{pmatrix} \sqrt{\epsilon} & 0 \\ 0 & 1 \end{pmatrix}. \tag{A6}$$

The Krauss gate $K(\epsilon)[\cdot] = \sum_{j=1}^2 K_j[\cdot]K_j^\dagger$ is a linear operation on a 2×2 matrix. Its eigenstates ψ_k and eigenvalues λ_k are $\psi_0 = |\uparrow\rangle\langle\uparrow|$, $\psi_1 = \sigma^z$, $\psi_2 = \sigma^+$, $\psi_3 = \sigma^-$, and $\lambda_0 = 1$, $\lambda_1 = \epsilon$, $\lambda_3 = \lambda_4 = \sqrt{\epsilon}$. On the other hand, the exponentiated Lindblad operator $e^{\Gamma t\,\mathcal{D}_{\sigma^-}}[\cdot]$ with $\mathcal{D}_L$ given by Eq. (8) has exactly the same eigenvectors $\{\psi_k\}$ and the eigenvalues $\mu_0 = 1$, $\mu_1 = e^{-\Gamma t}$, $\mu_2 = \mu_3 = e^{-\Gamma t/2}$. We thus obtain an application of a Krauss gate n times,

$$K^n(\epsilon)[\cdot] = e^{\Gamma t\,\mathcal{D}_{\sigma^-}}[\cdot], \quad \text{if } \epsilon = e^{-\Gamma t/n}. \tag{A7}$$

Analogously,

$$F^n(\epsilon)[\cdot] = e^{\Gamma t\,\mathcal{D}_{\sigma^+}}[\cdot], \quad \text{if } \epsilon = e^{-\Gamma t/n}. \tag{A8}$$

The boundary-driven Lindblad equation (7) is obtained in the limit

$$\tau = t/n \ll 1, \tag{A9}$$

$$U \approx I - i\tau P, \tag{A10}$$

$$\mathcal{M}[\rho(t)] \equiv \rho(t+\tau), \tag{A11}$$

so that $\lim_{\tau\to 0}(\mathcal{M}[\rho(t)] - \rho(t))/\tau = \frac{d\rho}{dt}$ after a straightforward algebra leads to differential equation (7). We thus can view the brick-wall unitary circuit as a Trotter discretization scheme of Lindblad Master equation (7).

The quantum Zeno limit corresponds to $\epsilon = 0$ in Eqs. (A5) and (A6), when the K and F gates are projecting the spins on pure states $|\downarrow\rangle$ and $|\uparrow\rangle$, respectively; i.e., $K[\cdot]$, $F[\cdot]$ become the so-called reset gates:

$$\sum_{j=1}^{2} F_j(0)\rho_{N+1}F_j(0)^\dagger = |\uparrow\rangle\langle\uparrow|, \quad \rho_{N+1} = \mathrm{tr}_{0,1,\ldots,N}\rho, \tag{A12}$$

$$\sum_{j=1}^{2} K_j(0)\rho_0 K_j(0)^\dagger = |\downarrow\rangle\langle\downarrow|, \quad \rho_0 = \mathrm{tr}_{1,\ldots,N,N+1}\rho. \tag{A13}$$

Indeed, an application of the K and F gates each elementary time step τ can be viewed as an effective realization of a protocol of repeated interactions, leading to the quantum Zeno regime. As a result, the quantum chain splits effectively in three parts: spin "0" (always in the state $|\downarrow\rangle\langle\downarrow|$) + internal spins $1, 2, \ldots, N$ + spin $N+1$ (always in the state $|\uparrow\rangle\langle\uparrow|$). The bulk interaction affecting the internal spins $1, 2, \ldots, N$

TABLE I. Numerical solutions of BAE (B1) and the entanglement NESS spectrum. Here $N = 5$, $M = 2$, and $\Delta = \frac{2}{3}$.

$p_1^{(\alpha)}$	$p_2^{(\alpha)}$	E	$\ln(\nu_\alpha/\nu_1)$
2.6041	2.0574	−6.6398	0
1.5086	2.6122	−4.5374	0.8315
1.5169	2.0803	−3.0687	1.2440
0.9512	2.6300	−2.4983	2.2403
0.4126	2.6596	−1.2134	4.4264
2.1192	0.9537	−1.1040	2.6273
0.4052	2.1843	0.0399	4.8052
0.9620	1.6082	0.8043	3.3183
1.7257	0.3885	1.7515	5.4714
$1.2864 + 0.8655i$	$1.2864 - 0.8655i$	1.8059	1.5936
$1.0386 + 0.2488i$	$1.0386 - 0.2488i$	2.8522	4.2450
0.3566	1.2991	3.4884	6.4596
0.7405	0.8791	4.1706	5.9499
0.9129	0.3134	4.9178	7.7571
0.2771	0.5625	5.8978	9.2974

gets renormalized, resulting in the application of the effective single spin boundary channels:

$$K_{\text{eff}}(\rho) = \text{tr}_1(U_{12}(|\downarrow\rangle\langle\downarrow| \otimes \rho)U_{12}^\dagger), \tag{A14}$$

$$F_{\text{eff}}(\rho) = \text{tr}_2(U_{12}(\rho \otimes |\uparrow\rangle\langle\uparrow|)U_{12}^\dagger), \tag{A15}$$

acting on spins 1 and N, respectively (see right-hand panel of Fig. 4).

The NESS for the brickwork circuit shown in Fig. 4 was recently analytically obtained by two co-authors of the present paper (see Ref. [22]). For the properly chosen target states and in the smaller Trotter time limit the spectrum of the NESS for the brickwork circuit [22] is indeed described by Eqs. (31) and (36) of the main text.

APPENDIX B: NUMERICAL EVIDENCE SHOWING CONSISTENCY OF EQ. (36)

For cases when $M > 1$, we currently lack full analytic proof of Eq. (36). Nevertheless, this equation can be verified numerically for $M = 2$ and larger M. The ratio ν_β/ν_α obtained

TABLE II. Numerical solutions of BAE (B1) and the entanglement NESS spectrum. Here $N = 6$, $M = 3$, and $\Delta = \frac{2}{3}$.

$p_1^{(\alpha)}$	$p_2^{(\alpha)}$	$p_3^{(\alpha)}$	E	$\ln(\nu_\alpha/\nu_1)$
2.1710	2.6609	1.6539	−9.4713	0
1.1143	2.1955	2.6721	−7.4769	1.1630
2.2510	0.5090	3.5861	−5.9674	3.3356
1.7101	1.1263	2.6760	−5.7429	1.7502
2.2068	1.7148	1.1306	−4.5789	2.0594
2.7009	1.8138	0.4928	−4.3896	3.9236
2.6694	$1.2008 + 0.6111i$	$1.2008 - 0.6111i$	−3.4460	1.7685
2.2621	0.4860	1.8187	−3.3285	4.2366
0.4550	1.3969	2.7080	−2.6780	4.8481
2.1861	$1.2128 - 0.6428i$	$1.2128 + 0.6428i$	−2.2398	1.9781
3.5856	$0.9363 - 0.1577i$	$0.9363 + 0.1577i$	−2.1442	4.0653
1.4017	2.2764	0.4486	−1.6501	5.1467
0.3894	1.0133	3.5639	−1.1651	6.1495
2.2529	$0.9381 - 0.1605i$	$0.9381 + 0.1605i$	−1.0633	4.3462
1.6596	$1.2492 - 0.7461i$	$1.2492 + 0.7461i$	−0.4221	2.2348
0.3843	1.0153	2.2998	−0.1800	6.4309
0.4343	1.8503	1.4124	−0.1772	5.6766
2.7341	0.6441	0.3290	−0.0218	7.7711
1.8046	$0.9432 + 0.1685i$	$0.9432 - 0.1685i$	0.5048	4.8354
0.3250	0.6419	2.3311	0.9047	8.0426
1.0197	1.8869	0.3738	1.2413	6.9218
1.0909	$1.3074 - 0.9403i$	$1.3074 + 0.9403i$	1.5866	2.6908
1.9386	0.3170	0.6368	2.2449	8.5127
1.3068	$0.9753 - 0.2139i$	$0.9753 + 0.2139i$	2.3009	5.5199
6.6372	1.4846	1.0309	2.8193	7.6528
0.5572	$1.3522 + 1.1229i$	$1.3522 - 1.1229i$	3.0105	3.8879
0.4728	$1.1858 - 0.5741i$	$1.1858 + 0.5741i$	3.7407	6.5804
0.3033	0.6254	1.5671	3.7418	9.2056
1.4664	$0.6801 + 0.4587i$	$0.6801 - 0.4587i$	3.9690	6.6551
0.3363	$1.0639 - 0.3143i$	$1.0639 + 0.3143i$	4.5199	8.4020
0.6724	$0.8847 - 0.0706i$	$0.8847 + 0.0706i$	4.8769	8.2448
0.5961	1.2358	0.2830	5.1327	10.1424
0.2880	$0.9049 - 0.1041i$	$0.9049 + 0.1041i$	5.4709	9.8548
0.2598	0.9604	0.5368	6.2627	11.2949
0.4815	0.7035	0.2388	7.1487	12.5699

from Eq. (36) consistently matches other approaches. Some explicit examples are shown in Tables I and II, for $M = 2$ and $M = 3$, where we employ the following BAE equivalent to Eq. (34):

$$e^{2i(N+1)p_j}\left[\frac{\Delta - e^{ip_j}}{1-\Delta e^{ip_j}}\right]^2 = \prod_{\sigma=\pm}\prod_{k\neq j}^{M}\frac{1-2\Delta e^{ip_j}+e^{ip_j}e^{i\sigma p_k}}{1-2\Delta e^{i\sigma p_k}+e^{ip_j}e^{i\sigma p_k}}, \quad j=1,\dots,M, \tag{B1}$$

and $\epsilon(p) = 4(\cos p - \Delta)$.

APPENDIX C: DERIVATION OF BETHE ANSATZ EQUATION (39)

The Hamiltonian of the spin-$\frac{1}{2}$ XYZ chain with generic open boundaries is

$$H = \sum_{\alpha=x,y,z}\sum_{n=1}^{N-1} J_\alpha \sigma_n^\alpha \sigma_{n+1}^\alpha + h_1 + h_N, \tag{C1}$$

$$h_1 = h_x^- \sigma_1^x + h_y^- \sigma_1^y + h_z^- \sigma_1^z, \tag{C2}$$

$$h_N = h_x^+ \sigma_N^x + h_y^+ \sigma_N^y + h_z^+ \sigma_N^z, \tag{C3}$$

where the boundary fields are parametrized as follows:

$$h_x^\mp = \pm\frac{\theta_1(\eta)}{\theta_4(0)}\prod_{l=1}^{3}\frac{\theta_4(\alpha_l^\mp)}{\theta_1(\alpha_l^\mp)}, \quad h_y^\mp = \mp i\frac{\theta_1(\eta)}{\theta_3(0)}\prod_{l=1}^{3}\frac{\theta_3(\alpha_l^\mp)}{\theta_1(\alpha_l^\mp)}, \quad h_z^\mp = \mp\frac{\theta_1(\eta)}{\theta_2(0)}\prod_{l=1}^{3}\frac{\theta_2(\alpha_l^\mp)}{\theta_1(\alpha_l^\mp)}. \tag{C4}$$

It has been proven in Ref. [21] that under the constraint

$$(N-1-2M)\eta = \sum_{\sigma=\pm}\sum_{k=1}^{3}\epsilon_k^\sigma\alpha_k^\sigma, \quad \prod_{k=1}^{3}\epsilon_k^\sigma = -1, \tag{C5}$$

the Bethe roots are given by the following two sets of Bethe Ansatz equations:

$$\text{Type I}: \quad \prod_{\sigma=\pm}\prod_{k=1}^{3}\frac{\theta_1\left(\mu_j-\epsilon_k^\sigma\alpha_k^\sigma-\frac{\eta}{2}\right)}{\theta_1\left(\mu_j+\epsilon_k^\sigma\alpha_k^\sigma+\frac{\eta}{2}\right)}\left[\frac{\theta_1\left(\mu_j+\frac{\eta}{2}\right)}{\theta_1\left(\mu_j-\frac{\eta}{2}\right)}\right]^{2N} = \prod_{\substack{k=1\\k\neq j}}^{M}\frac{\theta_1(\mu_j-\mu_k+\eta)\theta_1(\mu_j+\mu_k+\eta)}{\theta_1(\mu_j-\mu_k-\eta)\theta_1(\mu_j+\mu_k-\eta)}, \quad j=1,\dots,M, \tag{C6}$$

$$\text{Type II}: \quad \prod_{\sigma=\pm}\prod_{k=1}^{3}\frac{\theta_1\left(\nu_j+\epsilon_k^\sigma\alpha_k^\sigma-\frac{\eta}{2}\right)}{\theta_1\left(\nu_j-\epsilon_k^\sigma\alpha_k^\sigma+\frac{\eta}{2}\right)}\left[\frac{\theta_1\left(\nu_j+\frac{\eta}{2}\right)}{\theta_1\left(\nu_j-\frac{\eta}{2}\right)}\right]^{2N} = \prod_{\substack{k=1\\k\neq j}}^{N-1-M}\frac{\theta_1(\nu_j-\nu_k+\eta)\theta_1(\nu_j+\nu_k+\eta)}{\theta_1(\nu_j-\nu_k-\eta)\theta_1(\nu_j+\nu_k-\eta)} \quad j=1,\dots,N-1-M. \tag{C7}$$

It can be verified that, under the following configuration,

$$\{\alpha_1^-,\alpha_2^-,\alpha_3^-\} = \left\{\eta, \frac{1-\tau}{2}+iy_l, \frac{\tau}{2}+x_l-1\right\},$$
$$\{\alpha_1^+,\alpha_2^+,\alpha_3^+\} = \left\{\eta, \frac{\tau+1}{2}-iy_r, \frac{\tau}{2}+x_r\right\}, \tag{C8}$$

the boundary fields read

$$h_x^- = -\frac{\theta_2(iy_l)}{\theta_3(iy_l)}\frac{\theta_1(x_l)}{\theta_4(x_l)}J_x, \quad h_y^- = -i\frac{\theta_1(iy_l)}{\theta_3(iy_l)}\frac{\theta_2(x_l)}{\theta_4(x_l)}J_y, \quad h_z^- = -\frac{\theta_4(iy_l)}{\theta_3(iy_l)}\frac{\theta_3(x_l)}{\theta_4(x_l)}J_z,$$
$$h_x^+ = -\frac{\theta_2(iy_r)}{\theta_3(iy_r)}\frac{\theta_1(x_r)}{\theta_4(x_r)}J_x, \quad h_y^+ = -i\frac{\theta_1(iy_r)}{\theta_3(iy_r)}\frac{\theta_2(x_r)}{\theta_4(x_r)}J_y, \quad h_z^+ = -\frac{\theta_4(iy_r)}{\theta_3(iy_r)}\frac{\theta_3(x_r)}{\theta_4(x_r)}J_z. \tag{C9}$$

In addition, substituting Eq. (C8) into constraint (C5) and setting

$$\{\xi_1^-,\xi_2^-,\xi_3^-\} = \{-1,-1,-1\}, \quad \{\xi_1^+,\xi_2^+,\xi_3^+\} = \{-1,-1,1\},$$

yields the identity

$$(N+1-2M)\eta = x_r + iy_r - x_l - iy_r. \tag{C10}$$

By comparing Eqs. (C9) and (C10) with the results in the main text, we conclude that the Hamiltonian H_{D} defined in Eqs. (37) and (38) describes an *XYZ* chain with specifically constrained boundary fields. Its exact spectrum is then determined by the Bethe Ansatz equations of the form given in Eqs. (C6) and (C7).

As demonstrated in Ref. [20], the Hilbert space splits into two subspaces under the constraint in Eq. (C5). Based on the analogous result for the constrained open *XXZ* chain [16,18] and supporting numerical evidence, each set of Bethe Ansatz equations in Eqs. (C6) and (C7) is expected to correspond to one of these subspaces. The subspace we are interested in corresponds to Bethe Ansatz equations (C6). Substituting Eqs. (C8) into Eqs. (C6) yields

$$\left[\frac{\theta_1\left(u_j+\frac{\eta}{2}\right)}{\theta_1\left(u_j-\frac{\eta}{2}\right)}\right]^{2N+2}\frac{\theta_3\left(u_j+iy_l-\frac{\eta}{2}\right)}{\theta_3\left(u_j-iy_l+\frac{\eta}{2}\right)}\frac{\theta_4\left(u_j+x_l-\frac{\eta}{2}\right)}{\theta_4\left(u_j-x_l+\frac{\eta}{2}\right)}\frac{\theta_3\left(u_j-iy_r-\frac{\eta}{2}\right)}{\theta_3\left(u_j+iy_r+\frac{\eta}{2}\right)}\frac{\theta_4\left(u_j-x_r-\frac{\eta}{2}\right)}{\theta_4\left(u_j+x_r+\frac{\eta}{2}\right)}$$
$$=\prod_{\sigma=\pm1}\prod_{k\neq j}^{M}\frac{\theta_1(u_j+\sigma u_k+\eta)}{\theta_1(u_j+\sigma u_k-\eta)},\quad j=1,\ldots,M, \tag{C11}$$

which is Eq. (39).

APPENDIX D: NUMERICAL EVIDENCE SHOWING CONSISTENCY OF EQ. (43)

For the *XYZ* model, we are able to guess the analytic expression for the dissipatively dressed dispersion [Eq. (43)]. Some technical details followed by an explicit examples are given below.

Define the following state:

$$|\Psi(n_1,\ldots,n_M)\rangle=\bigotimes_{l_1=1}^{n_1}\psi(l_1)\bigotimes_{l_2=n_1+1}^{n_2}\psi(l_2-2)\cdots\bigotimes_{l_{M+1}=n_M+1}^{N}\psi(l_{M+1}-2M), \tag{D1}$$

$$\psi(x)=\begin{pmatrix}\bar{\theta}_1(\varepsilon+x\eta)\\-\bar{\theta}_4(\varepsilon+x\eta)\end{pmatrix},\quad \varepsilon=u_l=x_l+iy_l. \tag{D2}$$

Similarly to the *XXZ* case with *XY* plane boundary targeting, the set

$$|\Psi(n_1,\ldots,n_M)\rangle,\quad 0\leqslant n_1<n_2<\cdots<n_M\leqslant N,$$

forms a chiral invariant subspace of

$$H_D=\sum_{n=1}^{N-1}\vec{\sigma}_n\cdot\hat{J}\vec{\sigma}_{n+1}+h_1(\vec{n}_l)+h_N(\vec{n}_r), \tag{D3}$$

if special values of $\vec{n}_l,\vec{n}_r$ are chosen [see Eq. (38) in the main text].

One can use the chiral states (D1) to expand the Bethe state inside the invariant subspace and the corresponding expansion coefficients depend on the Bethe roots $\{u_1,\ldots,u_M\}$ in Eq. (39) [20].

Under the dynamics of the *XYZ* Hamiltonian, the Zeno NESS has reduced rank $d_M=\binom{N+1}{M}$, namely,

$$\rho_{\mathrm{NESS}}=\sum_{\alpha=1}^{d_M}\nu_\alpha|\alpha\rangle\langle\alpha|, \tag{D4}$$

where $|\alpha\rangle$ are eigenstates of H_D [Eq. (D3)] belonging to the chiral invariant subspace.

The operators $g_{l,r}$ can be written in terms of elliptic functions as follows:

$$g_l=G_L\otimes I^{\otimes_{N-1}},\quad g_r=I^{\otimes_{N-1}}\otimes G_R,$$
$$G_{L,R}=\begin{pmatrix}\frac{\theta_2(\eta)\sqrt{\theta_1(x_{l,r}-iy_{l,r})\theta_1(x_{l,r}+iy_{l,r})}}{\theta_4(x_{l,r})\theta_3(iy_{l,r})} & -\frac{\theta_1(x_{l,r}-iy_{l,r})[\theta_4(\eta)\theta_3(x_{l,r}+iy_{l,r})-\theta_3(\eta)\theta_4(x_{l,r}+iy_{l,r})]}{\theta_4(x_{l,r})\theta_3(iy_{l,r})\sqrt{\theta_1(x_{l,r}-iy_{l,r})\theta_1(x_{l,r}+iy_{l,r})}}\\ -\frac{\theta_1(x_{l,r}-iy_{l,r})[\theta_3(\eta)\theta_4(x_{l,r}+iy_{l,r})+\theta_4(\eta)\theta_3(x_{l,r}+iy_{l,r})]}{\theta_4(x_{l,r})\theta_3(iy_{l,r})\sqrt{\theta_1(x_{l,r}-iy_{l,r})\theta_1(x_{l,r}+iy_{l,r})}} & -\frac{\theta_2(\eta)\sqrt{\theta_1(x_{l,r}-iy_{l,r})\theta_1(x_{l,r}+iy_{l,r})}}{\theta_4(x_{l,r})\theta_3(iy_{l,r})}\end{pmatrix}. \tag{D5}$$

Similarly to the *XXZ* case, one can prove that all chiral states $|\Psi(n_1,\ldots,n_M)\rangle$ are eigenstates of g_l and g_r:

$$g_l|\Psi(s,n,m,\ldots)\rangle=(1-2\delta_{s,0})\kappa_l|\Psi(s,n,m,\ldots)\rangle, \tag{D6}$$

$$g_r|\Psi(n,m,\ldots,s)\rangle=(2\delta_{s,N}-1)\kappa_r|\Psi(n,m,\ldots,s)\rangle, \tag{D7}$$

$$\kappa_{l,r}=\frac{\sqrt{\theta_1(x_{l,r}-iy_{l,r})}}{\sqrt{\theta_1(x_{l,r}+iy_{l,r})}}\frac{\theta_1(\eta)\theta_2(x_{l,r}+iy_{l,r})}{\theta_4(x_{l,r})\theta_3(iy_{l,r})}. \tag{D8}$$

TABLE III. Numerical solutions of BAE (39) and the entanglement NESS spectrum. Here $\eta = 0.47$, $N = 5$, $M = 2$, $\tau = 0.35i$, $\{x_l, y_l\} = \{0.13, 0.21\}$.

$u_1^{(\alpha)}$	$u_2^{(\alpha)}$	E	ν_α/ν_1
$0.0532i$	$0.2393i$	-17.5382	1
$0.0532i$	$0.8950+0.1750i$	-16.0715	1.0877
$0.1106i$	$0.1050+0.1750i$	-15.5292	1.1215
$0.2972i$	$0.3050+0.1750i$	-3.2127	2.3593
$0.1100i$	$0.6950+0.1750i$	-2.6720	2.4323
$0.1050+0.1750i$	$0.3050+0.1750i$	-1.1998	2.6465
$0.3032i$	$0.5000+0.2451i$	0.7863	2.8787
$0.2668i$	$0.5000+0.2638i$	1.2244	2.9460
$0.7650+0.1643i$	$0.7650+0.1857i$	1.2589	3.0816
$0.1192i$	$0.5000+0.0645i$	1.6803	3.0172
$0.1050+0.1750i$	$0.5000+0.1174i$	2.7827	3.2291
$0.5000+0.0581i$	$0.1050+0.1750i$	3.1085	3.2729
$0.5000+0.2359i$	$0.3050+0.1750i$	15.6611	7.0102
$0.5000+0.0559i$	$0.6950+0.1750i$	15.9818	7.1036
$0.5000+0.1141i$	$0.5000+0.2941i$	19.9809	8.6736

Define the function

$$Q(x,\{y_k\}) = \prod_{k=1}^{M} \theta_1\left(x - y_k + \frac{\eta}{2}\right)\theta_1\left(x + y_k + \frac{\eta}{2}\right). \quad \text{(D9)}$$

Hypothesis D1. The spectrum ν_α of the Zeno NESS [Eq. (D4)] is given by

$$\frac{\nu_\beta}{\nu_\alpha} = \left|\frac{Q\left(\frac{1-\tau}{2}+iy_l,\{u_k^{(\alpha)}\}\right)Q\left(0,\{u_k^{(\beta)}\}\right)}{Q\left(0,\{u_k^{(\alpha)}\}\right)Q\left(\frac{1-\tau}{2}+iy_l,\{u_k^{(\beta)}\}\right)}\right|^2, \quad \text{(D10)}$$

where $\{u_j^{(\alpha)}\}$ and $\{u_j^{(\beta)}\}$ are the Bethe roots corresponding to $|\alpha\rangle$ and $|\beta\rangle$, respectively.

Analytic calculations for the *XYZ* model are extremely complicated due to the involvement of elliptic functions. Therefore, we resort to numerical calculations to verify our hypothesis.

Based on numerical results for the case $M = 1$, we find the following simple and elegant expression:

$$\frac{\nu_\beta}{\nu_\alpha} = \frac{w_{\alpha\beta}}{w_{\beta\alpha}} = \left|\frac{Q(b,u^{(\alpha)})}{Q(a,u^{(\alpha)})}\frac{Q(a,u^{(\beta)})}{Q(b,u^{(\beta)})}\right|^2, \quad \text{(D11)}$$

where a and b are two fixed system-dependent parameters. Some numerical data for the values of a and b are

τ	η	x_l	y_l	a	b
$0.35i$	0.47	0.16	0.05	0	$0.5-0.125i$
$0.35i$	0.47	0.71	0.05	0	$0.5-0.125i$
$0.35i$	0.47	0.16	0.67	0	$0.5+0.495i$
$0.35i$	0.47	0.16	0.49	0	$0.5+0.315i$
$0.35i$	0.47	0.16	0	0	$0.5-0.175i$
$0.35i$	0.55	0.16	0.05	0	$0.5-0.125i$
$0.49i$	0.47	0.16	0.75	0	$0.5+0.505i$

(D12)

On the base of numerics, we conclude that

$$a = 0, \quad b = \frac{1-\tau}{2} + iy_l.$$

For larger M, numerical results (see, e.g., Tables III and IV for an illustration) also indicate that

$$\frac{\nu_\beta}{\nu_\alpha} = \frac{w_{\alpha\beta}}{w_{\beta\alpha}} = \left|\frac{Q\left(\frac{1-\tau}{2}+iy_l,\{u_k^{(\alpha)}\}\right)Q\left(0,\{u_k^{(\beta)}\}\right)}{Q\left(0,\{u_k^{(\alpha)}\}\right)Q\left(\frac{1-\tau}{2}+iy_l,\{u_k^{(\beta)}\}\right)}\right|^2, \quad \text{(D13)}$$

where Q is given by Eq. (D9). Equation (D10) notably results in the dressed energy given by Eq. (43).

TABLE IV. Numerical solutions of BAE (39) and the entanglement NESS spectrum. Here $\eta = 0.47$, $N = 5$, $M = 3$, $\tau = 0.35i$, $\{x_l, y_l\} = \{0.13, 0.21\}$.

$u_1^{(\alpha)}$	$u_2^{(\alpha)}$	$u_3^{(\alpha)}$	E	ν_α/ν_{10}
$0.1050+0.1750i$	$0.1107i$	$0.2967i$	-26.4413	0.3315
$0.0520i$	$0.2412i$	$0.3650+0.1750i$	-11.1247	0.8185
$0.8954+0.1750i$	$0.3651+0.1750i$	$0.0520i$	-9.6473	0.8907
$0.6351+0.1750i$	$0.8946+0.1750i$	$0.2980i$	-9.6357	0.8914
$0.1088i$	$0.1046+0.1750i$	$0.6348+0.1750i$	-9.1113	0.9181
$0.1088i$	$0.6352+0.1750i$	$0.1054+0.1750i$	-9.1005	0.9187
$0.8950+0.1750i$	$0.0470i$	$0.5000+0.1076i$	-8.1303	0.9539
$0.5000+0.0900i$	$0.0846i$	$0.1050+0.1750i$	-7.6879	0.9765
$0.8950+0.1750i$	$0.6594+0.1750i$	$0.1294+0.1750i$	-7.6318	1.0058
$0.5000+0.0664i$	$0.8950+0.1750i$	$0.1194i$	-7.2318	1
$0.5000+0.1037i$	$0.0458i$	$0.3650+0.1750i$	7.2253	2.3593
$0.0819i$	$0.5000+0.2646i$	$0.3650+0.1750i$	7.6562	2.4135
$0.6350+0.1750i$	$0.2350+0.1636i$	$0.7650+0.1636i$	7.6989	2.5260
$0.3650+0.1750i$	$0.5000+0.0636i$	$0.1176i$	8.1122	2.4718
$0.5000+0.1164i$	$0.8952+0.1750i$	$0.3651+0.1750i$	9.2246	2.6469
$0.6351+0.1750i$	$0.1052+0.1750i$	$0.5000+0.1164i$	9.2304	2.6479
$0.6349+0.1750i$	$0.5000+0.0572i$	$0.1048+0.1750i$	9.5490	2.6825
$0.1052+0.1750i$	$0.3649+0.1750i$	$0.5000+0.0572i$	9.5566	2.6838
$0.1050+0.1750i$	$0.5000+0.0572i$	$0.5000+0.1163i$	11.0593	2.8735
$0.5000+0.1130i$	$0.5000+0.0551i$	$0.3650+0.1750i$	26.4301	7.1123

When $\tau \to +i\infty$, the *XYZ* model reduces to the *XXZ* model with $\{J_x, J_y, J_z\} \to \{1, 1, \cos(\pi\eta)\}$. By letting $iy_{l,r} = \frac{\tau}{2}$ and $\tau \to +i\infty$, the targeted boundary polarizations become

$$n^x_{l,r} = -\frac{\theta_2\left(\frac{\tau}{2}\right)}{\theta_3\left(\frac{\tau}{2}\right)}\frac{\theta_1(x_{l,r})}{\theta_4(x_{l,r})} = -\sin(\pi x_{l,r}),$$
$$n^y_{l,r} = -i\frac{\theta_1\left(\frac{\tau}{2}\right)}{\theta_3\left(\frac{\tau}{2}\right)}\frac{\theta_2(x_{l,r})}{\theta_4(x_{l,r})} = \cos(\pi x_{l,r}),$$
$$n^z_{l,r} = -\frac{\theta_4\left(\frac{\tau}{2}\right)}{\theta_3\left(\frac{\tau}{2}\right)}\frac{\theta_3(x_{l,r})}{\theta_4(x_{l,r})} = 0. \tag{D14}$$

The corresponding BAE [Eq. (39)] reduces to the trigonometric ones [18,23,24]

$$\left[\frac{\sin\left(\pi u_j + \frac{\pi\eta}{2}\right)}{\sin\left(\pi u_j - \frac{\pi\eta}{2}\right)}\right]^{2N+2}\left[\frac{\cos\left(\pi u_j - \frac{\pi\eta}{2}\right)}{\cos\left(\pi u_j + \frac{\pi\eta}{2}\right)}\right]^2 = \prod_{\sigma=\pm1}\prod_{k\neq j}^{M}\frac{\sin(\pi u_j + \sigma\pi u_k + \pi\eta)}{\sin(\pi u_j + \sigma\pi u_k - \pi\eta)}, \quad j = 1, \ldots, M. \tag{D15}$$

In conclusion, we retrieve the result of the previous section in the limit where $iy_{l,r} = \frac{\tau}{2}$ and $\tau \to +i\infty$.

[1] H. Bethe, Zur theorie der metalle, Z. Phys. **71**, 205 (1931).

[2] R. J. Baxter, *Exactly Solved Models in Statistical Mechanics* (Academic Press, London, 1982).

[3] L. A. Takhtadzhan and L. D. Faddeev, The quantum method of the inverse problem and the Heisenberg *XYZ* model, Russ. Math. Surv. **34**, 11 (1979).

[4] E. K. Sklyanin, L. A. Takhtadzhyan, and L. D. Faddeev, Quantum inverse problem method. I, Theor. Math. Phys. **40**, 688 (1979).

[5] E. K. Sklyanin, Separation of variables: New trends, Prog. Theor. Phys. Suppl. **118**, 35 (1995).

[6] V. Popkov, X. Zhang, C. Presilla, and T. Prosen, Bethe-Ansatz diagonalization of the steady state of boundary driven integrable spin chains, J. Phys. A: Math. Theor. **58**, 45LT01 (2025).

[7] J. Cao, S. Cui, W.-L. Yang, K. Shi, and Y. Wang, Spin-1/2 XYZ model revisit: General solutions via off-diagonal Bethe Ansatz, Nucl. Phys. B **886**, 185 (2014).

[8] Y. Wang, W.-L. Yang, J. Cao, and K. Shi, *Off-Diagonal Bethe Ansatz for Exactly Solvable Models* (Springer-Verlag, Berlin, Heidelberg, 2015).

[9] V. Popkov, D. Karevski, and G. M. Schütz, Driven isotropic Heisenberg spin chain with arbitrary boundary twisting angle: Exact results, Phys. Rev. E **88**, 062118 (2013).

[10] S. Attal and Y. Pautrat, From repeated to continuous quantum interactions, in *Annales Henri Poincaré* (Springer, 2006), Vol. 7, pp. 59–104.

[11] G. T. Landi, E. Novais, M. J. de Oliveira, and D. Karevski, Flux rectification in the quantum *XXZ* chain, Phys. Rev. E **90**, 042142 (2014).

[12] X. Mi, *et al.*, Stable quantum-correlated many-body states through engineered dissipation, Science **383**, 1332 (2024).

[13] P. Zanardi and L. C. Venuti, Coherent quantum dynamics in steady-state manifolds of strongly dissipative systems, Phys. Rev. Lett. **113**, 240406 (2014).

[14] V. Popkov, S. Essink, C. Presilla, and G. Schütz, Effective quantum Zeno dynamics in dissipative quantum systems, Phys. Rev. A **98**, 052110 (2018).

[15] E. K. Sklyanin, Boundary conditions for integrable quantum systems, J. Phys. A **21**, 2375 (1988).

[16] X. Zhang, A. Klümper, and V. Popkov, Phantom Bethe roots in the integrable open spin-$\frac{1}{2}$ XXZ chain, Phys. Rev. B **103**, 115435 (2021).

[17] V. Popkov and M. Salerno, Dissipative cooling towards phantom Bethe states in boundary-driven XXZ spin chain, Europhys. Lett. **140**, 11004 (2022).

[18] X. Zhang, A. Klümper, and V. Popkov, Chiral coordinate Bethe ansatz for phantom eigenstates in the open XXZ spin-$\frac{1}{2}$ chain, Phys. Rev. B **104**, 195409 (2021).

[19] E. T. Whittaker and G. N. Watson, *A Course of Modern Analysis* (Cambridge University Press, Cambridge, 1950).

[20] X. Zhang, A. Klümper, and V. Popkov, Invariant subspaces and elliptic spin-helix states in the integrable open spin-$\frac{1}{2}$ XYZ chain, Phys. Rev. B **106**, 075406 (2022).

[21] W.-L. Yang and Y.-Z. Zhang, *T–Q* relation and exact solution for the XYZ chain with general non-diagonal boundary terms, Nucl. Phys. B **744**, 312 (2006).

[22] V. Popkov and T. Prosen, Exact nonequilibrium steady state of *XXZ* circuits boundary driven with arbitrary resets or fields, Phys. Rev. Lett. **135**, 070401 (2025).

[23] J. Cao, H.-Q. Lin, K.-J. Shi, and Y. Wang, Exact solution of XXZ spin chain with unparallel boundary fields, Nucl. Phys. B **663**, 487 (2003).

[24] R. I. Nepomechie, Bethe ansatz solution of the open XXZ chain with nondiagonal boundary terms, J. Phys. A **37**, 433 (2004).